Introduction to Astrophysical Fluids

Lecture notes to MAS218

Axel Brandenburg & Wolfgang Dobler

Department of Mathematics
University of Newcastle upon Tyne

http://www.nordita.dk/~brandenb/teach/MAS218/notes.ps.gz

November 21, 2001

Table i: Some typical parameter values in geophysical and astrophysical settings.

	Adiabatic sound speed $c_{\rm s}^{(\rm ad)}$ $[\,{\rm km\,s^{-1}}]$	Density $\varrho\,[\,{\rm kg\,m^{-3}}]$	Kinematic viscosity $\nu\,[\,{\rm m^2\,s^{-1}}]$
Water	1.5	998	10^{-6}
Air	0.3	1.21	1.5×10^{-5}
Sun (surface)	10	10^{-3}	10^{-6}
Sun (interior)	300	10^{5}	10^{-2}
Galaxy	10..100	10^{-21}	10^{12}

Table ii: Some useful units used in astrophysics and the corresponding conversion into SI units.

1 Mm	=	10^6 m
1 AU	=	1.5×10^{11} m
1 pc	=	3.1×10^{16} m
$1\,M_\odot$	=	2.0×10^{30} kg
1 yr	=	3.2×10^{7} s
1 Myr	=	10^6 yr

Table iii: Radii of some celestial bodies.

Body	Radius
Earth	6 Mm
Jupiter	70 Mm
Sun	700 Mm
Accretion disc (CV)	10..1000 Mm
Galaxy	10 kpc $\approx 3\times10^{14}$ Mm

Table iv: Some common abbreviations.

AGN	Active galactic nucleus (plural: nuclei)
SN	Supernova (plural: supernovae)
SNR	Supernova remnant
BH	Black hole
WD	White dwarf (compact, degenerate star)
CV	Cataclysmic variable (unstable disc around WD)
HST	Hubble Space Telescope

Table v: Table of useful physical constants.

Quantity	Symbol	value	units
Newton's constant of gravity	G	6.673×10^{-11}	$\mathrm{m^3\,kg^{-1}\,s^{-2}}$
Stefan-Boltzmann constant	σ_{SB}	5.67×10^{-8}	$\mathrm{kg\,s^{-3}\,K^{-4}}$
Universal gas constant	$\mathcal{R}$	8315	$\mathrm{m^2\,s^{-2}\,K^{-1}}$
Speed of light	c	3×10^8	$\mathrm{m\,s^{-1}}$
Induction constant	μ_0	$4\pi \times 10^{-7}$	$\mathrm{V\,s\,A^{-1}\,m^{-1}}$

Table vi: A list of symbols and their meanings.

Ω	Omega	angular velocity
μ	mu	specific molecular weight
μ_0		induction constant

Chapter 1

Introduction

Astrophysics is concerned with phenomena in the sky that can be studied using mathematics and the law of physics. Many observed phenomena in the Universe are related to fluid dynamics and electromagnetism (stellar variability and rotation, solar sunspot cycle, stellar and galactic jets, galactic radio emission, cosmological expansion, etc). In this course, topics in modern astrophysical fluid dynamics will be discussed in order to obtain a conceptual understanding of the various processes involved. Their mathematical description will be introduced at an elementary level. The governing equations will be derived within the context they occur in.

1.1 Fluid dynamics

Fluid dynamics is the collective description of the flow of a large number of particles. Familiar examples of fluid dynamics include for example the flow of water in a river, surface waves in the sea, and of course the wind in the air. More complicated flow patterns on Earth are generated by obstructions due to solid bodies (buildings in a city, trees, etc). Other familiar examples of flows are free convection (updrafts above fields, downdrafts above lakes, but also the large scale atmospheric circulation).

In astrophysics the flow particles are not always neutral (molecules, atoms), but can be partially or fully ionised (electrons, ions, possibly mixed with neutrals). The forces acting on such particles are then not only pressure and gravity, but also the electromagnetic (or Lorentz) force.

Before we begin to describe fluid dynamical phenomena in astrophysics, let us first discuss the various astrophysical phenomena we see in the sky in a clear night. Not all of them will directly be relevant to fluid dynamics, at least not in the narrower sense. Also, some phenomena would rather be classified as geophysical fluid dynamics, but again, from a broader perspective they can also be relevant to astrophysics.

1.2 Examples of astrofluids in the sky

Let us think of some typical phenomena that everybody can observe, either with the naked eye or with a small telescope. We order them according to increasing distance from the Earth.

1. **The aurora**, or Northern lights, can be seen regularly in northern latitudes, but sometimes also further south, for example in Scotland.

2. **The Sun, sunspots, 11-year cycle, prominences**. In order to see some of those phenomena a little telescope or binoculars would help. Some big sunspot groups can sometimes also be seen with the naked eye at sunset when the Sun is not too bright. Also seen can be traces of the solar granulation, a convective flow pattern on the solar surface, but here one definitely needs a small telescope.

3. **Planets, Saturn's rings, Shoemaker-Levy crash onto Jupiter, Jupiter's red spot** are some topics related to our solar system. The following questions arise: how were the planets formed, what do Saturn's (and other giant planet's) rings tell us, why was it so difficult to predict the consequences of the comet crash on Jupiter, or what kept Jupiter's giant red spot together for so long?

4. **The zodiacal light** is a relict of the protostellar disc that surrounded the forming Sun and out of which planets formed. The zodiacal light can best be seen in the morning hours of the months October/November and the evening hours of February/March, when the ecliptic stands most steeply above the horizon.

5. **Meteors, meteorites, and comets** also tell us a lot about the solar system. Some meteorites are magnetised, which provides evidence that the early protostellar disc was magnetised when it cooled down below the *Curie point*, where ferromagnetic materials are able to hold a magnetic field. One particular meteorite has also been used as evidence of life on Mars, but this story now turned out to be a red herring.

6. **The Sun and other stars, variable stars, binaries, supernovae (SN), supernova remnants (SNR)** are examples in astrophysics where hydrodynamics and magnetic fields in stars play important roles. Stars may show complicated motions (circulation, granulation, oscillations), which can sometimes be very violent (supernovae). In other cases, they lead to magnetic field generation (the solar dynamo), which is the basis of solar and stellar activity, the sunspot cycle, prominences, and so on.

7. **The Milky Way**, ie our Galaxy, as well as other galaxies, are examples of astrophysical bodies on a much larger scale (ten orders of magnitude larger than the Sun). A lot of new physics is introduced by them which explains for example why galaxies can have a spiral structure, or why galaxies can have a halo of synchrotron emission. Many galaxies also show magnetic fields with a large scale pattern, reviving again the interest in dynamo theories. The Andromeda nebula is the brightest spiral galaxy visible with the naked eye.

8. **Interstellar clouds, HII nebulae, and reflection nebulae** are topics of galactic physics which touch to some extent upon questions of hydrodynamics: how do interstellar clouds form (this in turn is related to turbulence in the interstellar medium), and how can stars form out of clouds. HII nebulae are best seen on photographs using even an ordinary 50-mm lens. Exposure times of 5 min can be sufficient. The Orion nebula is the most dramatic one an can be seen with the naked eye.

9. **Open and globular clusters** are also members of our Galaxy which can be seen by the naked eye. With a somewhat broader understanding of what fluid dynamics is, they too belong to the subject. Clusters are selfgravitating bodies consisting of many stars. Similar to an ensemble of randomly moving gas particles in a star, the ensemble of stars too can provide some kind of a pressure that prevents the cluster from collapsing. The Pleiades are an example of a big nearby open cluster. M13 in the constellation of Hercules is a large globular cluster.

There are many more things that can now be seen, using the Hubble space telescope (HST) for example. Completely new classes of objects and phenomena have been discovered by employing other wavelengths of the electromagnetic spectrum (radio telescopes, as well as telescopes operating at microwave, infrared, ultraviolet, X-ray and gamma-ray wavelengths). Some events have been of particular interest quite recently:

- The *supernova SN1987A* provided essential information. Its neutrino emission was monitored, which led to new constraints regarding supernova explosions in general.
- The *crash of comet Shoemaker-Levy onto Jupiter* has been an unexpectedly dramatic event, which teaches us a lot about impacts of bodies in planetary atmospheres. Some of you may have seen the impact through a big telescope.
- The measurements of the cosmic background radiation by the *COBE satellite* have spawned a lot of new research in cosmology.
- The *Hubble Space Telescope* has provided direct images of objects whose existence has so far only been inferred theoretically. For example, accretion discs around protostars and in X-ray binaries are now observed directly. The outer rings of active galactic nuclei (AGN) have now also been seen directly.
- Ground-based telescopes provided evidence for an acceleration of cosmological expansion, thus calling into question the standard cosmological theories.

Table 1.1 gives an overview of the topics mentioned above, and which will be (or should have been) addressed in this course.

Table 1.1: Summary of topics

	Planets, Planetary systems	Stars, Binaries	Galaxies, AGNs, Clusters
Material	iron, lava	hydrogen, helium	gas, stars
Large scale flows	differential rotation	rotation and circulation	Keplerian flow, spirals
Discs, winds, jets	protoplanetary	around compact objects	AGNs, Quasars
Violent events	comet crash	SN explosions	starbursts, BH collisions
Flows & turbulence	circulation	convection	galactic rotation, SN explosions
Magnetic fields	compass, space crafts	cyclic fields	synchrotron emission

1.3 Units and symbols

Throughout this course we adopt SI units. However, most common in astrophysics are actually gaussian cgs units. In order to facilitate comparison with the literature we sometimes give some basic results in cgs units.

In addition to SI units we also use sometimes units that are appropriate in astrophysical context. For example distances in the solar system and in protostellar discs are often measured in astronomical units (1 AU is the average distance between the Sun and the Earth). On galactic scales one often measures distances in parsec or in kiloparsec. (The distance between the Sun and the centre of the Milky Way is approximately 10 kpc.) Time is sometimes conveniently measured in years ($1\,\mathrm{yr} = 3.16 \times 10^7\,\mathrm{s}$), and mass is expressed in units of solar masses ($1\,M_\odot = 2 \times 10^{30}\,\mathrm{kg}$).

See Table ii for a list of such units and Table v for some frequently needed fundamental constants.

When we use cartesian coordinates we denote them (x, y, z). For cylindrical polar coordinates we use (ϖ, ϕ, z), and for spherical polar coordinates we use (r, θ, ϕ).

Typically we end up using a bunch of greek symbols in places. However, not all funny symbols are greek. The symbol ϖ is a mixture between pi (π) and omega (ω), and is therefore sometimes called 'pomega'. Table vi shows a list of some other symbols and their meanings.

1.4 The equation of motion

At the basis of mechanics lies the *equation of motion* describing the motion of a single particle or an ensemble of particles (and a gas is an ensemble of molecular or atomic particles) under the influence of external forces. The equation of motion is also known as Newton's first law and can be written as

$$m\frac{d\mathbf{v}}{dt} = \mathbf{F}, \tag{1.1}$$

where d/dt denotes time differentiation, $\mathbf{v}$ is the velocity vector and $\mathbf{F}$ is the force acting on the particle of mass m. Table 1.2 gives examples of forces.

Table 1.2: Table of forces that can govern the motion of a single particle of mass m, electric charge q, radius r, volume V, in the presence of gravity $\mathbf{g}$, a magnetic field $\mathbf{B}$, overall rotation $\mathbf{\Omega}$, in a medium of dynamical viscosity μ, and density ϱ.

Name	symbol		expression
gravity force	$\mathbf{F}_{\rm g}$	$=$	$m\mathbf{g}$
electrostatic force	$\mathbf{F}_{\rm el}$	$=$	$q\mathbf{E}$
Lorentz force	$\mathbf{F}_{\rm L}$	$=$	$q\mathbf{v}\times\mathbf{B}$
Coriolis force	$\mathbf{F}_{\rm Cor}$	$=$	$-m\mathbf{\Omega}\times\mathbf{v}$
centrifugal force	$\mathbf{F}_{\rm c}$	$=$	$m\Omega^2\boldsymbol{\varpi}$
Stokes drag force	$\mathbf{F}_{\rm D}$	$=$	$-6\pi\mu r\mathbf{v}$
turbulent drag force	$\mathbf{F}_{\rm D}^{\rm (turb)}$	$=$	$-C_{\rm D}\pi r^2\varrho v^2\hat{\mathbf{v}}$
buoyancy force	$\mathbf{F}_{\rm buoy}$	$=$	$\Delta\varrho V\mathbf{g}$

1.5 Text books

Some useful text books include:

Shore, S. N. 1992 *An Introduction to Astrophysical Hydrodynamics.* Academic Press.

Shu, F. H. 1992 *The Physics of Astrophysics. Vol. II. Gas Dynamics.* University Science Books, Sausalito, California.

Zeilik, M. 1994 *Astronomy: The Evolving Universe.* John Wiley & Sons.

The book by Zeilik has many pictures and explains things qualitatively (no formulae). The book by Shore is more mathematical and interesting to read. It has many misprints however. Finally, the book by Shu covers things in much more detail. Regarding accretion discs good books are those by Frank et al (1992) and Campbell (1997):

Campbell, C. G. 1997 *Magnetohydrodynamics in Binary Stars.* Kluwer Academic Publishers, Dordrecht.

Frank, J., King, A. R., & Raine, D. J. 1992 *Accretion Power in Astrophysics.* Cambridge: Cambridge Univ. Press.

As for solar physics, the book by Stix is quite comprehensive:

Stix, M. 1989 *The Sun: An Introduction.* Springer.

Chapter 2

Particle flows and atmospheric dynamics

Again, we start with phenomena closed to us. We mentioned already the aurora, which is just 100 km above us, provided we are in the right latitudes or otherwise just lucky enough. The aurora results from a complicated interaction of the Earth's magnetic field with the solar wind. Therefore we mention the origin of the Earth's magnetic field first.

2.1 The Earth

2.1.1 Ionosphere and magnetosphere

Thirty years ago, when the American space craft Explorer flew high enough into the upper layers of the Earth's atmosphere, they discovered a belt with very energetic particle radiation. These belts are now called the van Allen radiation belts. In fact, certain magnetic field configurations can trap particles (magnetic bottle). These ionised particles then form the *ionosphere*.

The Earth atmosphere plays the role of a TV screen, it starts to emit light when electrons ionise or excite N_2 and/or O_2. The final acceleration is due to strong electric fields high in the atmosphere at a height of a few thousand kilometers. Initially, however, the particles are set into motion because of field aligned currents that are produced in the magnetosphere. Those currents are driven by plasma motions in the magnetotail and occur when the magnetotail goes unstable. This instability in turn is caused by changes in the solar wind, especially when the magnetic field of the solar wind turns south, i.e. in the opposite direction as the Earth's magnetic field, facilitating thus reconnection.

Magnetospheres, ie magnetised envelopes shielded against the ambient solar wind, occur around all planets that have a magnetic field. Also strongly magnetised stars, such as neutron stars, have magnetospheres. We won't go further into this right now. Instead we shall now consider the motion of a charged particle in a magnetic field in more detail. After that we shall consider another case of particle motion where the governing force is not the magnetic field, but gravity together with friction.

2.1.2 Spiralling along field lines

Electrically charged particles spiral along magnetic field lines. If the particle's motion is only governed by the magnetic force, the equation of motion is

$$m\frac{d\mathbf{v}}{dt} = q\mathbf{v} \times \mathbf{B}, \tag{2.1}$$

where m is the mass of the particle (electron, proton, etc) and q is its charge (negative for an electron). This effect may be familiar from the technique of a TV tube, where an electron beam is deflected according to Eq. (2.1); see Figure 2.1.

The magnetic field is now assumed to be constant and along the z-direction (in a local coordinate system), $\mathbf{B} = (0, 0, B)$, so

$$\mathbf{v} \times \mathbf{B} = \begin{pmatrix} v_x \\ v_y \\ v_z \end{pmatrix} \times \begin{pmatrix} 0 \\ 0 \\ B \end{pmatrix} = \begin{pmatrix} +v_y B \\ -v_x B \\ 0 \end{pmatrix}, \tag{2.2}$$

and therefore

$$\begin{aligned} m\dot{v_x} &= +qv_y B\ , & (2.3)\\ m\dot{v_y} &= -qv_x B\ , & (2.4)\\ m\dot{v_z} &= 0, & (2.5) \end{aligned}$$

where the dots denote time differentiation, ie $\dot{\mathbf{v}} \equiv d\mathbf{v}/dt$, and the solution is

$$\begin{aligned} v_x &= v_{\phi 0}\cos(\omega_g t + \Phi)\ , & (2.6)\\ v_y &= -v_{\phi 0}\sin(\omega_g t + \Phi)\ , & (2.7)\\ v_z &= v_{z0} & (2.8) \end{aligned}$$

where

$$\omega_g = \frac{qB}{m} \tag{2.9}$$

is the *gyration frequency* or *cyclotron frequency*. The integration constants Φ (the phase) and $v_{\phi 0}$, v_{z0} follow from the initial conditions. The corresponding trajectories are given by

$$\begin{aligned} x &= x_0 + \frac{v_{\phi 0}}{\omega_g}\sin(\omega_g t + \phi)\ , & (2.10)\\ y &= y_0 + \frac{v_{\phi 0}}{\omega_g}\cos(\omega_g t + \phi)\ , & (2.11)\\ z &= z_0 + v_{z0}t & (2.12) \end{aligned}$$

with three more integration constants x_0, y_0, z_0. These equations define a helical spiral of constant radius and pitch.

2.1.3 The magnetic bottle and magnetic drift

If the field is not uniform, the motion will no longer follow perfect spirals. Two different things can happen. If the field strength increases along the direction of the magnetic field, the gyration frequency will increase, so the particle will spin faster. However, the particle has only a certain

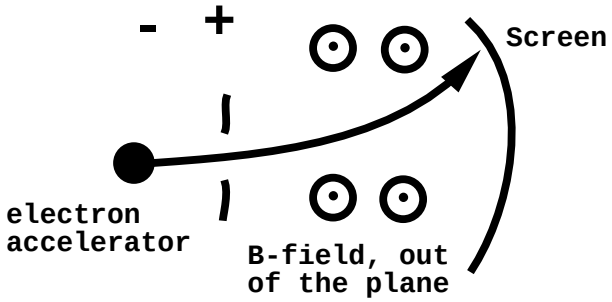

Figure 2.1: Electron path in a TV tube. Deflection of an electron beam by a magnetic field. The field points out of the paper. The term $\mathbf{v} \times \mathbf{B}$ points downwards but, because electrons have negative charge, the beam is deflected upwards.

amount of energy and there is therefore a limit how fast it can go. Having reached this limit, the particle cannot go any further into the regions of stronger field strength and has therefore to return. This property allows the particle to be trapped in a magnetic flux tube whose ends are closed by having enhanced field strength there. Such an arrangement is also called a magnetic bottle.

Magnetic bottles play a role in confining plasma in fusion experiments. The dipole magnetic field of the Earth also provides effectively a magnetic bottle, because towards the poles the field becomes strong, causing particles to be reflected back into the region of weaker field. The result of a numerical integration of Eq. (2.1) is shown in Figure 2.2, where a dipolar field has been assumed with $\mathbf{B} = \boldsymbol{\nabla} \times (A\hat{\boldsymbol{\phi}})$ and $A = \sin\theta/r^2$, where r is spherical radius and θ is colatitude.

Figure 2.2 shows yet another effect, namely a drift of the particle perpendicular to the direction of the field and perpendicular to the direction in which the field strength varies. This leads to a drift of the particle in the longitudinal direction. The reason is simple. When the particle spirals along the field, the part of the arc where the field is stronger is tighter than the part of the arc where the field is weaker. This leads to a mismatch which causes the drift.

2.1.4 The Earth's magnetic field

The Earth's magnetic field is dipole-like, tilted 12° against the rotation axis, and it has reversed polarity 9 times in the past 3.5 Myr in an irregular fashion. (1 Mega-year is 10^6 yr.) Since the field is not constant, and because the conductivity is too poor to keep currents going for long enough, there must be some mechanism (a dynamo) that converts kinetic energy (from convection in the outer iron core) into magnetic energy and thus replenishes the magnetic field continuously. The key ingredients of such a mechanism are differential rotation and cyclonic motions, see the box below.

The self-exited dynamo: differential rotation winds up an initially poloidal magnetic field and generates a toroidal magnetic field. As we will explain later, magnetic field lines are often strongly coupled to the fluid and can therefore be dragged along by the fluid motion, provided the field is not too strong to resist this process. A toroidal magnetic field in turn can generate new poloidal magnetic field (needed in the first place) by convection in the presence of rotation. A downdraft starts to swirl because of the overall rotation (Coriolis force) similar to lows and highs on a weather map.

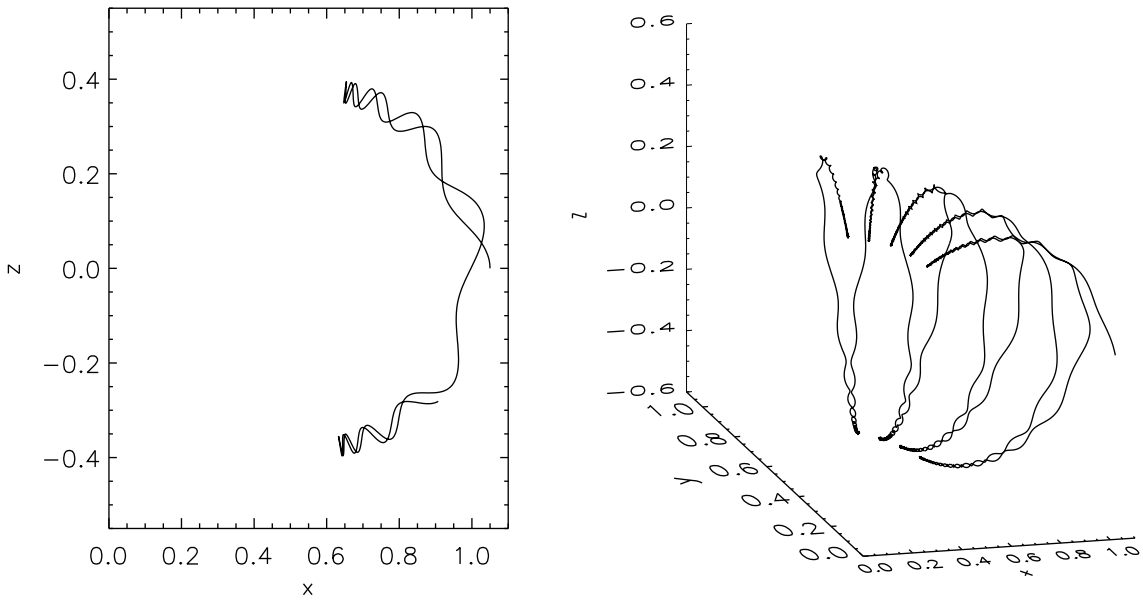

Figure 2.2: Left: plot of a particle path in the dipole magnetic field of the Earth. Note the reflection near the two poles where the field strength increases and therefore the gyration radius decrease. Right: three-dimensional visualisation of the particle trajectory. Note a drift of the magnetic field perpendicular the magnetic field gradient, ie in the azimuthal direction.

2.2 Particle settling in the atmosphere

Let us still stay on Earth with our examples and consider the ejecta of a volcano some years after the eruption. We want to know how long it takes for little micrometer-sized particles to settle to the surface. In fact, up to 10 years after the eruption of Krakatau (a volcanic island in the sea between Sumatra and Java that erupted violently in 1883) there were luminous clouds visible 45 min after sunset.

Geometric optics after sunset: near the equator, 45 min after sunset, the Sun is about $\alpha = 10°$ below the horizon. (24 h corresponds to 360°, so 0.75 h corresponds to $0.75 \times 360°/24 = 10°$.) Since the dust clouds are still illuminated by the Sun, their height must be $H = (1/\cos\alpha - 1)\, R_E \approx 120\,\mathrm{km}$; see Figure 2.3.

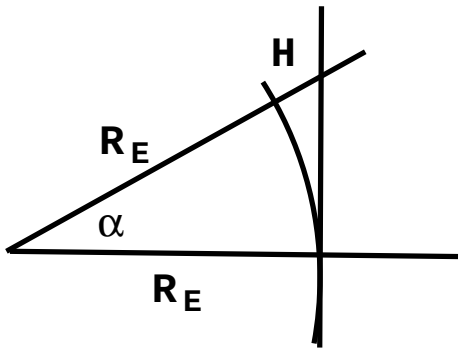

Figure 2.3: 45 min after sunset the Sun still illuminates dust particles in 100 km height.

The reason those dust particles can stay for such a long time in the atmosphere is because of friction or a viscous drag force $F_{\rm D}$. In the absence of friction, the free fall time, $t=\sqrt{2H/g}$ would be about 160 s. Now in the presence of friction, the equation of motion is

$$m\frac{dv}{dt}=-mg+F_{\rm D}, \tag{2.13}$$

where the drag force $F_{\rm D}$ can be computed from the full hydrodynamical equations under the assumption that nonlinear terms are unimportant. The result is called Stokes' drag with

$$F_{\rm D}=-6\pi\mu r v, \tag{2.14}$$

where μ is the dynamical friction $\mu=2\times10^{-5}\,{\rm kg\,m^{-1}\,s^{-1}}$ for air, r the radius of the particles, m its mass, and v its velocity. Initially the particle will just accelerate, but fairly quickly friction sets in and the terminal velocity is reached, which results from the balance

$$0=-\frac{4\pi}{3}r^3\varrho_{\rm p}g-6\pi\mu r v, \tag{2.15}$$

where the particle mass is replaced by its volume times its density which, for rocks and silicates, is about $4\times10^3\,{\rm kg\,m^{-3}}$. So, for $r=1\mu{\rm m}=10^{-6}\,{\rm m}$ we obtain

$$|v|=\frac{2}{9}\frac{r^2\varrho_{\rm p}g}{\mu}\approx4\times10^{-4}\,{\rm m/s}. \tag{2.16}$$

So, the descent time from a height of $H=100\,{\rm km}$ is then $t=H/|v|\approx3\times10^8\,{\rm s}=10\,{\rm yr}$.

We shall return to this type of algebra later in connection with the formation of planetesimals out of the dust in the protosolar nebula. Before this, we shall briefly discuss thermal buoyancy, which we just encountered in connection with the volcano eruption.

2.3 Flows in the atmosphere

The dust particles are not simply tossed out into the air by the volcano, but they can rise along with the heated air into high altitude. This raises the following question. Consider a fluid parcel that is heated by a certain amount. How far would it rise before it returns back, for example. Or does it return back? In order to answer those questions let us first consider the effect of the buoyancy force.

2.3.1 The buoyancy force: the hot air balloon as an example

Gas motions in the Earth's and solar atmospheres are often driven by buoyancy. As an example we now calculate the buoyancy force from a hot air balloon. The buoyancy force results from a lower density inside the balloon (or any other container) and the density outside it. So the buoyancy force is given by

$$F_{\rm buoy}=-\Delta\varrho Vg, \tag{2.17}$$

where g is the gravitational acceleration ($\approx10\,{\rm m\,s^{-2}}$), and $\Delta\varrho=\varrho_{\rm i}-\varrho_{\rm e}$ is the density difference between the interior and the exterior of the balloon. If the density within the balloon is smaller than outside, $\Delta\varrho<0$ and $F_{\rm buoy}$ is positive. The density deficit depends on the temperature

excess and, assuming that there is no pressure difference (which is justified for a hot air balloon), the two are proportional to each other, so

$$\frac{\Delta\varrho}{\varrho} = -\frac{\Delta T}{T}. \tag{2.18}$$

Let us assume that the temperature inside the balloon is $80^\odot$ C and the exterior temperature is $20^\odot$ C. The temperature difference is then $60^\odot\,\mathrm{C} = 60\,\mathrm{K}$, and the *absolute* temperature is then is $T = 20\,\mathrm{K} + 273\,\mathrm{K} \approx 300\,\mathrm{K}$ (Kelvin), so

$$\frac{\Delta\varrho}{\varrho} = -\frac{60}{300} \approx 0.2. \tag{2.19}$$

So, one cubic meter of hot air is about 20% lighter than cold air. Since the density of air is approximately $\varrho = 1\,\mathrm{kg\,m^{-3}}$ we have $\Delta = 0.2\,\mathrm{kg\,m^{-3}}$. The larger the balloon, the more hot air there is and the lighter is the balloon. Assuming a spherical shape with radius R the volume of the balloon is $V_{\mathrm{balloon}} = (4\pi/3)R^3$, so the upward force of the entire balloon is

$$(-\Delta\varrho)gV = \frac{4\pi}{3}R^3(-\Delta\varrho)g. \tag{2.20}$$

This has to be balanced against the weight of the balloon, which is mg, if m is the mass of the payload. Thus, we have

$$\frac{4\pi}{3}R^3\Delta\varrho = m. \tag{2.21}$$

If we want to know the size of the balloon necessary to carry, say, $m = 500\,\mathrm{kg}$, we have

$$R = \left(\frac{3}{4\pi}\,\frac{m}{\Delta\varrho}\right)^{1/3} \approx \left(\frac{1}{4}\,\frac{500\,\mathrm{kg}}{0.2\,\mathrm{kg\,m^{-3}}}\right)^{1/3} = \sqrt[3]{625}\,\mathrm{m} \approx 9\,\mathrm{m}, \tag{2.22}$$

which seems quite plausible.

2.3.2 The perfect gas. Equation of state

We need an equation of state that relates the pressure p of a gas to its density ϱ and its temperature T. For a perfect gas this relation is

$$p = \frac{\mathcal{R}}{\mu}T\varrho, \tag{2.23}$$

where $\mathcal{R} = 8315\,\mathrm{m^2\,s^{-2}\,K^{-1}}$ (this is a script or curly R!) is the universal gas constant and μ is the molecular weight (dimensionless), which is the atomic or molecular mass expressed in units of 1 amu (to a good approximation, $\mu_{\mathrm{H}} \approx 1$). The quantity $\mathcal{R}T/\mu$ has the dimensions of a velocity squared. As we will see later, this quantity equals the square of the sound speed in a situation where changes in the pressure and density are isothermal.[1]

The quantity

$$c_{\mathrm{s}}^{(\mathrm{isoth})} = \left(\frac{\mathcal{R}T}{\mu}\right)^{1/2} \tag{2.24}$$

[1] When the changes are adiabatic, e.g. when thermal conduction is weak, the sound speed is slightly larger: $c_{\mathrm{s}} = \sqrt{\gamma}c_{\mathrm{s}}^{(\mathrm{isoth})}$.

is therefore also referred to as the *isothermal* sound speed. For air the value of μ is 28.8, so

$$c_{\rm s}^{\rm (isoth)} \approx \left(\frac{8315 \times 300}{28.8}\right)^{1/2} {\rm m/s} \approx 300\,{\rm m/s} \tag{2.25}$$

For ionised hydrogen $\mu = 0.5$ (the atomic mass is 1 and the number of particles 2, because there are protons and electrons). However, in the Sun, as well as elsewhere in the cosmos, there is also helium and the value of μ is then around 0.6. On the other hand, the presence of neutral and molecular hydrogen increases the average value. Approximate values (to an order of magnitude) of $c_{\rm s}^{\rm (isoth)}$ and T are given in Table 2.1.

Table 2.1: Typical sound speeds in the Sun.

T	$c_{\rm s}^{\rm (isoth)}$
10^2 K	1 km/s
10^4 K	10 km/s
10^6 K	100 km/s

Specific heats: The energy content of a gas is measured by its specific heat, which is the energy needed to increase the temperature by one degree. This quantity can be measured by holding either the volume of the gas constant (specific heat at constant volume, c_v) or by keeping the pressure constant (specific heat at constant pressure, c_p). In general, the specific heat at constant volume is smaller than the specific heat at constant pressure, because when the pressure is constant the energy is not only used to increase the temperature, but also to increase the volume. The work associated with this is $p\,\Delta V = \mathcal{R}/\mu \Delta T$, and therefore

$$c_p - c_v = \frac{p\,\Delta V}{\Delta T} = \mathcal{R}/\mu \tag{2.26}$$

According to the kinetic theory of gases (ie the theory that describes the gas as noninteracting particles) the specific heat at constant volume is equal to $\mathcal{R}/(2\mu)$ times the number of degrees of freedom f of a single particle (atom or molecule), ie $c_v = f\mathcal{R}/(2\mu)$. Because of Eq. (2.26) we have $c_p = (f+2)\mathcal{R}/(2\mu)$. Therefore the ratio of the two specific heats, $\gamma \equiv c_p/c_v$, is equal to

$$\gamma = \frac{f+2}{f}. \tag{2.27}$$

For a mono-atomic gas $f = 3$, corresponding to the three directions of translation, so $\gamma = 5/3 = 1.67$. Further, for a bi-atomic (dumbbell-like) molecule there are two additional degrees of freedom corresponding to the rotation of the molecule about the axis connecting the two atoms and perpendicular to it, so $f = 3+2$ and $\gamma = 7/5 = 1.4$. The third rotation axis is only distinguished in molecules with more than two atoms. So, for example in CO_2 $f = 6$ and therefore $\gamma = 8/6 = 4/3 \approx 1.33$. Yet, values of γ closer to unity are possible when the molecules exhibit various kinds of oscillations that further increase the number of degrees of freedom.

2.3.3 The isothermal atmosphere

Things are changing as we rise. The exterior density decreases, decreasing therefore the buoyancy force. On the other hand, the pressure decreases, so the balloon (or gas parcel) expands and so the interior density also decreases. Which one decreases faster, depends on the temperature profile in the atmosphere. The simplest type of atmosphere is the isothermal atmosphere, ie one where the temperature is constant.

In any atmosphere in hydrostatic (or mechanical) equilibrium the weight (per unit area) of a thin layer of gas, $\varrho g dz$, increases the pressure by the amount $p_{\rm top} - p_{\rm bot} = -\Delta p = \varrho g dz$, so the condition of hydrostatic equilibrium is

$$\frac{dp}{dz} = -\varrho g, \tag{2.28}$$

where g is the gravitational acceleration ($\approx 10\,\mathrm{m/s^2}$ for the Earth and $\approx 300\,\mathrm{m/s^2}$ at the solar surface).

If the atmosphere is isothermal, then $p = c_{\rm s}^2 \varrho$, where $c_{\rm s}^2 = \text{const}$. In that case we obtain

$$\frac{d}{dz}(c_{\rm s}^2 \varrho) = c_{\rm s}^2 \frac{d\varrho}{dz} = -\varrho g \tag{2.29}$$

or (after dividing by ϱ and $c_{\rm s}^2$)

$$\frac{1}{\varrho}\frac{d\varrho}{dz} = \frac{d\ln\varrho}{dz} = -g/c_{\rm s}^2 = \text{const}, \tag{2.30}$$

so

$$\ln\varrho = -gz/c_{\rm s}^2 + \ln\varrho_0, \tag{2.31}$$

where $\ln\varrho_0$ is an integration constant.

So, ϱ decreases exponentially with height, ie

$$\varrho = \varrho_0 e^{-z/H}, \tag{2.32}$$

where

$$H = c_{\rm s}^2/g \tag{2.33}$$

is also called the *scale height* of the atmosphere.

Furthermore, since $p = c_{\rm s}^2 \varrho$ we have

$$p = p_0 e^{-z/H}, \tag{2.34}$$

where $p_0 = c_{\rm s}^2 \varrho_0$.

2.3.4 Adiabatic changes. Entropy

If a fluid parcel preserves its heat content, ie if radiative losses or other heating mechanisms are unimportant, pressure and density changes are said to be *adiabatic*. This is described by a

quantity called the entropy which is then unchanged. For a perfect gas, we define the specific entropy (ie entropy per unit mass) as

$$s = c_v \ln p - c_p \ln \varrho. \tag{2.35}$$

(In principle there could be an additive constant s_0, but we can put it to zero, because only *changes* in s matter.) The entropy per unit mass is relevant, because we consider a bubble of a given mass. The specific entropy, in units of c_p, is

$$s/c_p = \frac{1}{\gamma} \ln p - \ln \varrho \equiv \frac{1}{\gamma} \ln \left(p/\varrho^\gamma \right), \tag{2.36}$$

so if changes in p and ϱ are adiabatic, ie if $s = \text{const}$, then

$$p = e^{\gamma s/c_p} \varrho^\gamma \tag{2.37}$$

or

$$\frac{p}{p_0} = \left(\frac{\varrho}{\varrho_0} \right)^\gamma \tag{2.38}$$

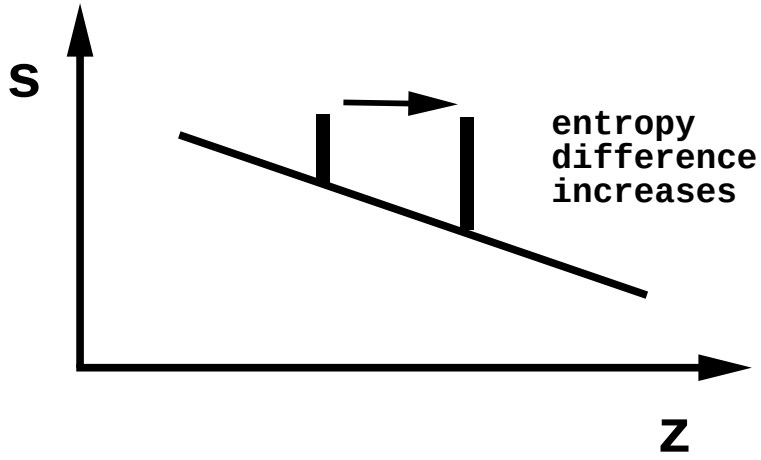

Figure 2.4: Entropy profile for an unstable atmosphere. The entropy difference between the bubble and the exterior increases constantly as the bubble ascends.

In order to understand the evolution of a parcel in an atmosphere it is convenient to compute the vertical dependence of s. For an isothermal atmosphere the vertical gradient is

$$\frac{1}{c_p} \frac{ds}{dz} = -\frac{1}{\gamma H} + \frac{1}{H} = \frac{\gamma - 1}{\gamma} \frac{1}{H} > 0, \tag{2.39}$$

so s increases with height. This means that a rising fluid parcel, whose entropy is conserved, will end up in a location where the surrounding entropy is higher. At the same time, however, the pressure inside and outside the bubble will be the same, so $p_\mathrm{i} - p_\mathrm{e} \equiv \Delta p = 0$, where subscripts i and e refer to interior and exterior values. Thus, from Eq. (2.36) we have

$$\Delta s/c_p = -\Delta \ln \varrho. \tag{2.40}$$

So, since the rising fluid parcel ends up in a location of higher exterior entropy, we have $\Delta s < 0$ and therefore $\Delta \ln \varrho > 0$, so the fluid parcel becomes *heavier* and will be pulled back by the gravity. This provides a restoring force proportional to the vertical displacement, which leads to

2.3.5 Brunt-Väisälä oscillations

When the bubble rises over a distance z (from its original position, where $\Delta s = 0$), the relative change of density $\Delta\varrho/\varrho = \Delta \ln \varrho$ between interior and exterior is equal to

$$\Delta \ln \varrho = -\Delta s/c_p = +\frac{1}{c_p}\frac{ds}{dz}z, \tag{2.41}$$

so it is proportional to the displacement z. Now the buoyancy force acting on the fluid parcel per unit volume, is $-\Delta\varrho\, g$, so

$$\varrho\ddot{z} = -\Delta\varrho\, g \tag{2.42}$$

(dots indicate differentiation with respect to time), or [2]

$$\ddot{z} = -\frac{\Delta\varrho}{\varrho}g = -g\,\Delta \ln \varrho = g\,\frac{\Delta s}{c_p} = -\frac{g}{c_p}\frac{ds}{dz}\,z. \tag{2.43}$$

A solution of this differential equation is

$$z = z_0 \cos(\omega_{\rm BV} t), \tag{2.44}$$

where z_0 is the initial displacement from the equilibrium state and $\omega_{\rm BV}$ is the Brunt-Väisälä (or buoyancy) frequency (sometimes also called $N_{\rm BV}$) with

$$\omega_{\rm BV}^2 = \frac{g}{c_p}\frac{ds}{dz}. \tag{2.45}$$

This expression only makes sense if the atmosphere is stably stratified, ie if $\mathbf{g}\cdot\boldsymbol{\nabla}s < 0$, and so we can express (2.45) in vector notation,

$$\omega_{\rm BV}^2 = -\mathbf{g}\cdot\boldsymbol{\nabla}s/c_p. \tag{2.46}$$

2.3.6 Polytropic atmospheres

Real atmospheres are not isothermal. A better approximation is to assume that T increases linearly with depth. (See Chapter 3.2.) *Warning*: depth increases downwards, whereas height increase upwards. To distinguish between the two we denote depth by $\tilde{z}$, with $\tilde{z} = z_{\rm max} - z$. Thus, $dz = -d\tilde{z}$, and therefore Eq. (2.28) becomes

$$\frac{1}{\varrho}\frac{dp}{d\tilde{z}} = g. \tag{2.47}$$

Now for a polytropic atmosphere we have

$$T/T_0 = \tilde{z}/H_T, \tag{2.48}$$

where H_T is the temperature scale height, the value of which will be determined below. The density is then assumed to be a power law of T, so

$$\varrho/\varrho_0 = (T/T_0)^m, \tag{2.49}$$

[2] The change in sign in the last equation may be counter-intuitive, but one should keep in mind that

$$\Delta s = s_{\rm i} - s_{\rm e} = s(z{=}0) - s(z) = \frac{ds}{dz}\cdot(0 - z) = -\frac{ds}{dz}z\,.$$

where m is the polytropic index. Because of Eq. (2.23) the pressure is then

$$p/p_0 = (T/T_0)^{m+1}. \tag{2.50}$$

Plugging this into (2.47) we have

$$\varrho_0^{-1}(z/H_T)^{-m}\frac{d}{d\tilde{z}}\left[p_0(z/H_T)^{m+1}\right] = g \tag{2.51}$$

or

$$\frac{\mathcal{R}T_0}{\mu H_T}(m+1) = g. \tag{2.52}$$

The (constant) temperature gradient is then

$$\beta \equiv T_0/H_T = \frac{g}{(m+1)\mathcal{R}/\mu}. \tag{2.53}$$

In order to see what happens to our fluid blob we determine again the entropy gradient, using Eq. (2.36),

$$\frac{1}{c_p}\frac{ds}{dz} = -\frac{1}{c_p}\frac{ds}{d\tilde{z}} = -\frac{m+1}{\gamma\tilde{z}} + \frac{m}{\tilde{z}} = \frac{1}{\tilde{z}}\frac{(\gamma-1)m-1}{\gamma}. \tag{2.54}$$

Here we have used the fact that $d\ln p/dz = d\ln(p/p_0)/d\tilde{z}$, because the second term in $\ln(p/p_0) = \ln p - \ln p_0$ is constant, and so

$$\frac{d\ln p}{d\tilde{z}} = \frac{d\ln(p/p_0)}{d\tilde{z}} = (m+1)\frac{d\ln(T/T_0)}{d\tilde{z}} = (m+1)\frac{d\ln\tilde{z}}{d\tilde{z}} = \frac{m+1}{\tilde{z}}. \tag{2.55}$$

Evidently, for

$$m < \frac{1}{\gamma-1} \tag{2.56}$$

the entropy gradient ds/dz turns negative, so a rising blob would find itself in an environment whose entropy is getting smaller and smaller as it rises further. This means its density relative to the exterior density is getting smaller and smaller, so the bubble becomes even more unstable. Since such bubbles may break lose all over the place the whole medium will start to bubble. This process is called convection. In this case the Brunt-Väisälä frequency becomes formally imaginary, corresponding to an exponentially growing solution. This is because $\cos\omega_{\rm BV}t = \mathrm{Re}\left(e^{-i\omega_{\rm BV}t}\right) = e^{\sigma_{\rm BV}t}$, where $\sigma_{\rm BV} = \mathrm{Im}(\omega_{\rm BV})$. For $\gamma = 5/3$ the criterion (2.54) for instability is $m < 3/2$ (or $m > 5/2$ for $\gamma = 7/5$ and $m > 3$ for $\gamma = 4/3$).

We shall return to convective instability in connection with the solar convection zone; see Figure 3.2.

2.4 The Jovian Planets

Talking of *Jovian planets* one normally means Jupiter, Saturn, Uranus, and Neptune. These planets are also called *giant planets*, because their radii are $5-10$ times that of the Earth. Their average density is around $(0.7-1.6)\times10^3\,\mathrm{kg/m^3}$, as opposed to $(4-6)\times10^3\,\mathrm{kg/m^3}$ for the terrestrial planets (Mercury, Venus, Earth and Mars).

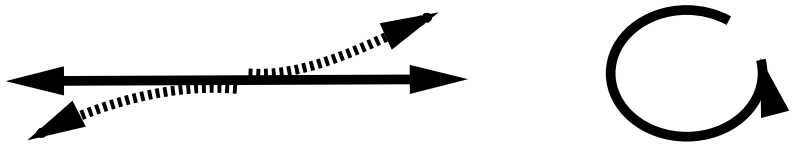

Figure 2.5: Foucault pendulum: *want to change sense of plot, so that it applies to northern hemisphere.* The pendulum swing back and forth tries to keep its orientation in space. The earth moves under it in the counter-clockwise direction, which makes the direction of the pendulum appear to turn in the clockwise direction.

A prominent hydrodynamical phenomenon on Jupiter is the Great Red Spot. It has an elliptical shape and is about 14 Mm × 40 Mm in size, ie larger than the Earth! It is basically a region of high pressure and very stable (we know about its existence for at least 400 yr). It is located on the southern hemisphere where it rotates counterclockwise, as expected from the action of the Coriolis force; see the box below. Its revolution time is about 7 days, which is long compared to the rotation period of Jupiter of just 10 hours.

The Coriolis force. It is often convenient to consider the governing equations in a *rotating* frame of reference. When performing a coordinate transformation from a non-rotating to a rotating frame of reference, an extra force appears in the equation of motion. (An example of such a coordinate transformation was given in the course MAS215 on Planetary Orbits.) Thus, the equation of motion takes the form

$$\frac{d\mathbf{u}}{dt} = ... - 2\mathbf{\Omega} \times \mathbf{u}, \tag{2.57}$$

where the dots refer to the terms that we had before also. The Earth's rotation can be established by using a pendulum (the Foucault pendulum). Assume that we are on the north pole, so $\mathbf{\Omega} = (0, 0, \Omega)$, and that the pendulum swings in the x direction, ie $\mathbf{u} = (u_x, 0, 0)$, then the Coriolis force is $-2\mathbf{\Omega} \times \mathbf{u} = -(0, 2\Omega u_x, 0)$. After a short time τ the pendulum experiences a force in the negative y direction when the pendulum swings forward ($u_x > 0$) and in the negative y direction when it swings backwards. After one day the plane in which the pendulum swings back and forth has rotated by $360^c irc.$ This an be understood by viewing the Earth as rotating underneath the pendulum; see Figure 2.5. An important effect of the Coriolis force is to cause converging flow regions to swirl counterclockwise. Those are the regions of low pressure, as seen on a weather map; see Figure 2.6. For such a motion, the Coriolis force (pointing inwards) balances the outwards directed pressure force. High pressure regions, on the other hand, rotate clockwise. This is the case for Jupiter's red spot.

Jupiter has a magnetic field that is 10 times as strong as the Earth's magnetic field (4×10^{-4} T). Jupiter also has a magnetosphere and auroras in higher latitudes. The Jovian magnetic field is probably also generated by a hydromagnetic dynamo, but now it is liquid metallic hydrogen which conducts the currents.

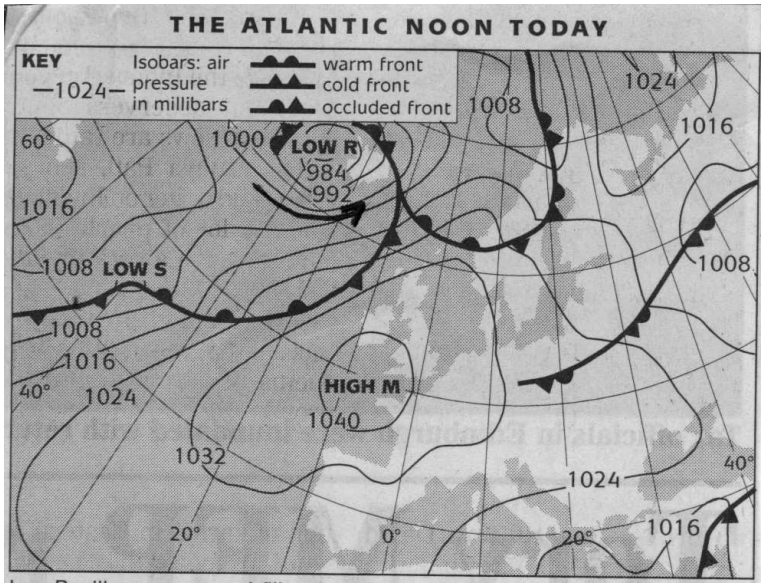

Figure 2.6: The action of the Coriolis force: low pressure regions are converging, and then the Coriolis force makes them swirl in the counter-clockwise direction (or clockwise direction on the southern hemisphere).

2.5 The pressure-less collapse

The gravitational acceleration due to a point mass is in general given by

$$\mathbf{g} = -\frac{GM}{r^3}\mathbf{r}. \tag{2.58}$$

In the following we adopt spherical polar coordinates, so the radial component of the gravitational force is $-GM/r^2$.

2.5.1 Free-fall collapse of a homogeneous sphere

Consider a spherical molecular cloud of constant density ϱ_0. Let us first assume there is nothing to prevent it from collapsing, i.e. pressure and magnetic fields are assumed to be negligible. The equation of motion then reduces to the form

$$\ddot{r} = -\frac{GM}{r^2}, \tag{2.59}$$

where r is, as usual, the spherical radius, ie the distance from the centre of mass. The mass M inside the sphere of initial radius r_0 is $(4\pi/3)r_0^3\varrho_0$, so we obtain

$$\frac{\ddot{r}}{r_0} = -\frac{4\pi}{3}G\varrho_0\left(\frac{r}{r_0}\right)^{-2} \tag{2.60}$$

We may nondimensionalise by defining $\xi = r/r_0$ and $\tau = t/t_0$, where $t_0 = [(4\pi/3)G\varrho_0]^{-1/2}$. Thus we have

$$\ddot{\xi} = -\xi^{-2}, \tag{2.61}$$

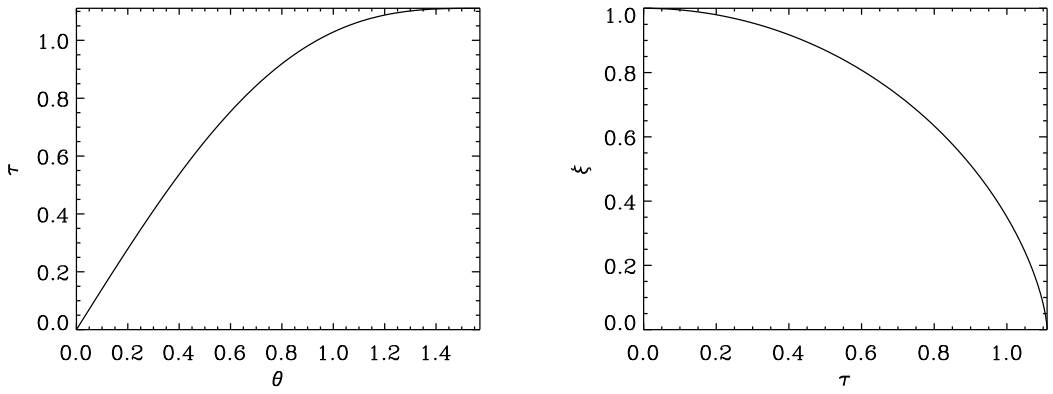

Figure 2.7: Solution of the homogeneous collapse problem.

where the dot now denotes differentiation with respect to τ. We multiply by $\dot{\xi}$ and integrate (note that $d\xi^{-1}/d\tau = -\dot{\xi}\xi^{-2}$)

$$\tfrac{1}{2}\dot{\xi}^2 = \xi^{-1} - 1, \tag{2.62}$$

where the integration constant is put to unity, because $\dot{\xi} = 0$ initially when $\xi = 1$. It is convenient to define a new variable θ via

$$\xi = \cos^2\theta, \tag{2.63}$$

so

$$\dot{\xi} = -2\dot{\theta}\sin\theta\cos\theta, \quad \xi^{-1} - 1 = \sin^2\theta/\cos^2\theta, \tag{2.64}$$

so we are left with

$$2\dot{\theta}^2\cos^2\theta = \cos^{-2}\theta \tag{2.65}$$

which can be integrated

$$\int \cos^2\theta d\theta = 2^{-1/2}\tau + \text{const.} \tag{2.66}$$

The integral can be looked up in a table:

$$\tfrac{1}{2}\theta + \tfrac{1}{4}\sin 2\theta = 2^{-1/2}\tau, \tag{2.67}$$

which can easily be verified. The integration constant is zero, because $\theta = 0$ for $\tau = 0$. The solution is plotted in Figure 2.7.

We define the free-fall time $\tau_{\rm ff}$ as the time it takes for the sphere to collapse to $\xi = 0$, ie $\theta = \pi/2$. This time is $\tau = \pi/\sqrt{8} \approx 1.11$ or, in physical units,

$$t_{\rm ff} = \sqrt{\frac{3\pi}{32G\varrho_0}} \tag{2.68}$$

Note that the free-fall time is independent of r_0, and depends just on the initial density ϱ_0. Therefore, all shells collapse at the same time to the origin. Plugging in the mean interstellar density $\varrho = 2 \times 10^{-21}\,\mathrm{kg\,m^{-3}}$, we have $t_{\rm ff} = 5 \times 10^7\,\mathrm{yr}$. The density can be ~ 10 times shorter if a hundred times larger density is assumed, which is indeed the case in interstellar clouds.

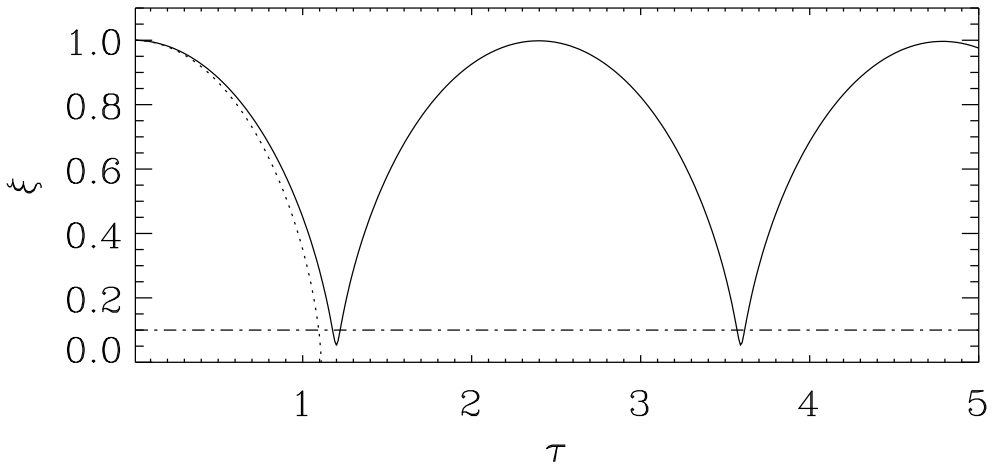

Figure 2.8: Collapse calculation with centrifugal force with $\ell^2/(GMr) = 0.1$. The dotted line gives the solution for $\ell = 0$ and the dotted-dashed line gives the equilibrium value, $r_{\rm eq} = \ell^2/(GM)$.

2.5.2 Free-fall collapse with rotation

In the presence of rotation we have to take the centrifugal force into account,

$$F_{\rm centrif} = m\Omega^2 r, \tag{2.69}$$

where Ω is the angular velocity. As the collapse progresses, the radius decreases, and so the body will spin up like a pirouette dancer. This is because angular momentum is conserved. The angular momentum is given by

$$\ell = \Omega^2 r \tag{2.70}$$

and so if $\ell = {\rm const}$ then we can rewrite the centrifugal force as

$$F_{\rm centrif} = m(\Omega^2 r^4)\, r^{-3} = m\ell^2 r^{-3}. \tag{2.71}$$

Thus, Eq. (2.59) has an additional term,

$$\ddot{r} = -\frac{GM}{r^2} + \frac{\ell^2}{r^3}. \tag{2.72}$$

Figure 2.8 gives a numerical solution, which shows that the collapse stops and reverses in an oscillatory way. In reality we won't expect such oscillations to occur, because this would require coherent motion of all particles within one ring. More realistic is that each particle goes on an elliptic orbit instead. Nevertheless, the main thing is that rotation does prevent the final collapse. The only way to proceed with the collapse is by having a mechanism that removes angular momentum. There are two possibilities: magnetic fields and turbulent viscosity. They will be discussed later.

2.5.3 The effect of gas pressure

In the presence of gas pressure, there will eventually be a balance between gas pressure and gravity. If the overall mass involved is anywhere between 0.1 and 10 solar masses, a star of that

mass will form. If the mass is greater than 10 solar masses the configuration is likely to break up into smaller pieces, and multiple stars may form, for example. If the mass is too small (less than $\sim 0.1\,M_\odot$) the configuration will never become hot enough to ignite and will form a brown dwarf.

Stars are really in a state of balance between gas pressure and gravity. However, any perturbation to this state results in oscillations. Those oscillations can be spherically symmetric, in which case they are called *radial pulsations*, but in the more general case they are non-spherically symmetric. Their frequency is a multiple of $\sqrt{G\overline{\varrho}}$, which is thus similar to the inverse free-fall time. Because the restoring force is the pressure gradient, those modes are in general referred to as *p-modes*. Those modes play an important role in astrophysics, especially in solar physics, because their frequencies depend on the average sound speed in various parts of the Sun and can actually be used to infer the variation of the sound speed (and therefore the temperature) with depth. We return to this in the section on helioseismology (§ 3.5).

2.6 Protostellar discs

The solar system, like other planetary systems, has formed out of a spinning cloud, also called the protosolar nebula. There are however various problems and the details of the explanation are more complicated.

2.6.1 Angular momentum transport

There is a problem regarding the angular momentum distribution. Although the Sun contains 99.9% of the mass of the solar system, it holds only 1% of the angular momentum. So there must have been a mechanism that removes angular momentum from the inner parts and deposits it in the outer parts. One such mechanism could be magnetic fields. Suppose the early Sun already had a magnetic field, and suppose also that the protoplanetary nebula was sufficiently hot for the matter to be ionised, then the field would couple shells at different radii, so the inner shells tend to be slowed down and the outer shells tend to be spun up. Obviously, all this must have happened early on before the planets formed, because the magnetic field only couples to the gas (charged particles), but not to the planets.

2.6.2 Formation of planets: the qualitative picture

There are three main mechanisms that contribute to the growth of planets: gravitational contraction, accretion and condensation. The whole process begins with little micrometer-sized grains that collide and stick together to form larger-pebble sized bodies. This process is similar to the growth of snowflakes. Once they are formed they quickly fall to the midplane of the disc; see Figure 2.9. Then gravitational attraction can take over and accumulate the pebbles to form planetesimals of a few kilometers to a few hundred kilometers in size. This whole process of planetesimal formation with sizes of a few hundred kilometers may last only a few 10^4 yr. These bodies continue to feed themselves by pulling lighter neighbouring bodies by gravitation and so sweep clear a strip of material in the surroundings of forming protoplanets. The terrestrial planets have grown to the present size in about 10^8 yr. This clearing out of a region around each protoplanet must have been responsible for the spacing of the planets that we see now.

The chemistry of the terrestrial planets is governed by the temperature at which they formed. Mercury formed at a temperature of about 1400 K, Venus 900 K, the Earth at 600 K, Mars at 400 K and Jupiter at 200 K. The hotter the material from which planetesimals condensed, the heavier the dominant elements. For example Mercury has a larger iron core than the Earth.

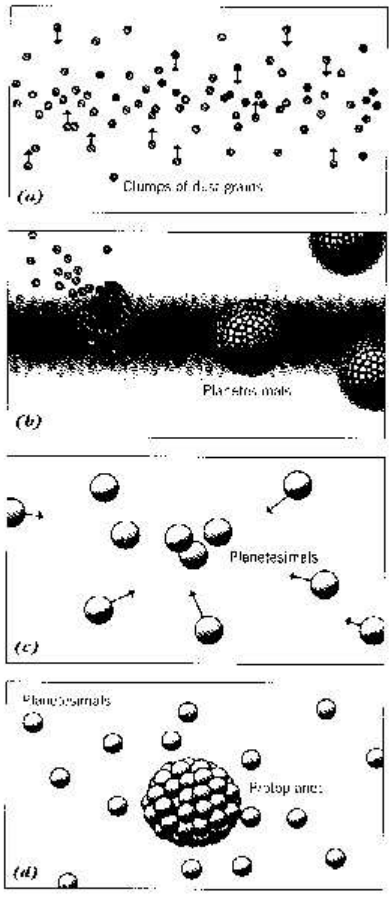

FIGURE 12.22 Possible scenario for the formation of the planets. (*a*) Dust grains collide and stick to form small objects that fall into a thin disk. (*b*) Gravity pulls these together to make asteroidal-sized bodies, the planetesimals. (*c*) The planetesimals collect in clusters to form the cores of the protoplanets (*d*), which evolve into the planets.

Figure 2.9: Sketch illustrating the formation of planetesimals and planets in the protosolar nebula. (Taken from Zeilik's book.)

At some point, around an age of 10^5 to 10^6 yr the protosun must have ignited. Intense radiation pressure and strong solar wind will have pushed the remaining gas out of the solar system. Only heavier gases remained captured by the gravity of the planets.

The formation of Jupiter may have been entirely different. It is possible that Jupiter formed by gravitational attraction alone. In the beginning Jupiter was much hotter, because the release of gravitational energy could have heated Jupiter to about 1000 K. Thus, during the formation of the Galilean satellites the dominant elements may have mimicked a similar chemical sequence as the terrestrial planets.

2.6.3 Particle dynamics in a disc potential

Assuming now cylindrical polar coordinates, $\mathbf{r} = (\varpi, \phi, z)$, where ϖ is the distance from the rotation axis and z the distance from the midplane. The gravitational potential is $\phi = -GM/r = -GM/\sqrt{\varpi^2 + z^2}$, so the gravitational force is

$$\mathbf{g} = -\boldsymbol{\nabla}\phi = \frac{GM}{r^3}\begin{pmatrix} -\varpi \\ 0 \\ -z \end{pmatrix}. \tag{2.73}$$

The radial component of gravity is balanced by the centrifugal force, $\Omega^2\varpi$, so

$$\frac{GM}{r^3}\varpi = \Omega^2\varpi, \tag{2.74}$$

or, cancelling out ϖ,

$$\frac{GM}{r^3} = \Omega^2, \tag{2.75}$$

The force is therefore

$$\mathbf{g} = \Omega^2 \begin{pmatrix} -\varpi \\ 0 \\ -z \end{pmatrix}. \tag{2.76}$$

In particular the vertical component of gravity is thus

$$g_z = -\Omega^2 z. \tag{2.77}$$

In the vertical direction a particle is governed by the z dependent gravity force, $g_z = -\Omega^2 z$. This affects both the gas as well as dust grains. The resulting stratification of the gas will be considered in § 5.2. Here we consider the effects on dust particle. The vertical component of the equation of motion of a particle, Eq. (2.13), is then

$$m\frac{dv}{dt} = -mg_z + F_{\rm D}. \tag{2.78}$$

In protostellar discs, however, the mean-free path of the gas particles causing the friction is so long that the usual Stokes formula (2.14) has to be modified and is therefore instead

$$F_{\rm D} = -\varrho c_{\rm s} a^2 \dot{z}, \tag{2.79}$$

where a is the radius of the particle and $c_{\rm s}$ is the ambient sound speed. Using $\dot{z} = v$ for the velocity of the particle and $m = (4\pi/3)\varrho_{\rm p} a^3$ for its mass, we can rewrite (2.78) as

$$\ddot{z} + \tau_p^{-1}\dot{z} + \Omega^2 z = 0, \tag{2.80}$$

where

$$\tau_p = \frac{4\pi}{3}\frac{\varrho_{\rm p}}{\varrho}\frac{a}{c_{\rm s}} \tag{2.81}$$

is the damping time. The characteristic equation,

$$\lambda^2 + \tau_p^{-1}\lambda + \Omega^2 z = 0, \tag{2.82}$$

has two solutions. For small values of $\tau_p\Omega$ the two solutions are $\lambda_1 = \tau_p^{-1}$ and $\lambda_2 = \tau_p\Omega^2$, so the solution to (2.80) can be written as

$$z = \frac{H}{1-\Omega^2\tau_p^2}\left[e^{-\Omega^2\tau_p t} - \Omega^2\tau_p^2 e^{-t/\tau_p}\right] \tag{2.83}$$

where H is the initial height of the particle. This solution satisfies $\dot{z}(t=0) = 0$.

2.6.4 Sweeping up particles in the midplane

When all the mass has accumulated near the midplane, it is likely to get very crowded near the midplane. Since neighbouring orbits have different orbital speeds, the particles will eventually collide. One can work out that this will happen when the bodies have grown to a size of 30 km.

However, if the bodies are on exactly circular orbits the collision time is pretty long. If a is the radius of the body and r the orbital radius then the orbital periods on the orbits $r \pm a$ are

$$P_{1,2} = 2\pi\sqrt{\frac{r^3}{GM}}\left(1 \pm \frac{3}{2}\frac{a}{r}\right) \tag{2.84}$$

In order that the period difference, $\Delta P = P_1 - P_2$, becomes equal to the period itself one has to wait $N = P/\Delta P = r/(3a)$ orbits. For 30 km sized bodies and $r = 1\,\mathrm{AU} = 150 \times 10^6\,\mathrm{km}$ (solar neighborhood) one has to wait for about 10^6 orbits, ie 10^6 yr, because the orbital period in the solar neighborhood is 1 year.

Chapter 3

The Sun (and other stars)

In this chapter, we explicitly discuss only the Sun. This is mainly because for the Sun a lot of details are observable and known that are much more difficult to obtain for distant stars. Apart from this "selection effect", all the concepts presented here are applicable to broad classes of stars and in this sense, the Sun appears only as a representative of stars in general.

3.1 The energy budget of the Sun

The luminosity of the Sun is $L_\odot = 4 \times 10^{26}\,\mathrm{W}$. The total interception with the Earth is

$$\frac{\pi R_E^2}{4\pi R_{E\odot}^2} = 4 \times 10^{-10}, \tag{3.1}$$

where R_E is the radius of the Earth (6400 km) and $R_{E\odot}$ is the distance between the Earth and the Sun ($= 1\,\mathrm{AU} = 1.5 \times 10^{11}$ m). So the total power reaching the Earth is $4 \times 10^{-10} \times 4 \times 10^{26}\,\mathrm{W} = 1.6 \times 10^{17}\,\mathrm{W}$, which is still a lot compared with the total energy consumption in the US, which is $10^{13}\,\mathrm{W}$.

The total thermal energy content of the Sun is approximately

$$E_\mathrm{th} = \int c_v T \varrho \, dV \approx M c_\mathrm{s}^2 \approx 2 \times 10^{30}\,\mathrm{kg}\,\left(10^5\,\mathrm{m/s}\right)^2 = 2 \times 10^{40}\,\mathrm{J} \tag{3.2}$$

The time it would take to use up all this energy to sustain the observed luminosity is the Kelvin-Helmholtz time

$$\tau_\mathrm{KH} = E_\mathrm{th}/L_\odot = 10^6\,\mathrm{yr} \tag{3.3}$$

which is long compared to time scales we could observe directly, but short compared with the life time of the Sun and the solar system (more like $5 \times 10^9\,\mathrm{yr}$). This led to the discovery of the nuclear energy source of stars. One sometimes defines the Kelvin-Helmholtz time scale as the ratio of *potential* energy to luminosity, but thermal and potential energy are quite similar (Virial theorem). In fact, this similarity can be used to estimate the central temperature of a star by equating $GM/R = \mathcal{R}T_c/\mu$. For the Sun this gives

$$T_c = \frac{\mu}{\mathcal{R}}\frac{GM}{R} = \frac{0.6}{8300}\,\frac{7 \times 10^{-11}\,2 \times 10^{30}}{7 \times 10^8}\,\mathrm{K} = \frac{3}{4}\,10^{-4}\,10^{-11}\,2 \times 10^{22}\,\mathrm{K} = 1.5 \times 10^7\,\mathrm{K} \tag{3.4}$$

for its central temperature. This estimate is actually spot on. It also tell us that the central temperature of the Sun is only determined by its mass and radius, and not, as one might have expected, by the effectiveness of the nuclear reactions taking place there.

3.2 Energy transport and convection

In the central parts of the Sun, energy is transported by photon diffusion: the optical mean-free path is short compared with other relevant length scales (eg pressure scale height), so we can make the diffusion assumption, by which the radiative flux $\mathbf{F}_{\rm rad}$ points from hot regions to cooler regions and is proportional to the temperature gradient, ie

$$\mathbf{F}_{\rm rad} = -K\boldsymbol{\nabla}T \tag{3.5}$$

where

$$K = \frac{16\sigma_{\rm SB}T^3}{3\kappa\varrho} \tag{3.6}$$

is the radiative conductivity, κ the opacity, and $\sigma_{\rm SB}$ the Stefan-Boltzmann constant. The value of κ, and therefore of K, depends on the atomic physics involved in absorbing and scattering photons. It changes slowly, so to a first approximation, $\boldsymbol{\nabla}T$ = const. In a plane parallel atmosphere dT/dz = const, ie T increases *linearly* with depth, which leads to the polytropic atmosphere considered in § 2.3.6.

A good approximation for the opacity κ is given by Kramer's formula

$$\kappa = \kappa_0\varrho T^{-7/2}, \tag{3.7}$$

where $\kappa_0 = 6.6\times10^{18}\,{\rm m^5\,K^{7/2}\,kg^{-2}}$. This value may well be up to 30 times larger if the gas is "metal rich", ie a good electron supplier, so that bound-free processes become important as well. In practice, a good value is $\kappa_0 \approx 10^{20}\,{\rm m^5\,K^{7/2}\,kg^{-2}}$. With this coefficient and Kramer's formula, the conductivity is

$$K = \frac{16\sigma_{\rm SB}T^{13/2}}{3\kappa_0\varrho^2}. \tag{3.8}$$

If the stratification is given by a polytrope, $\varrho\sim T^m$, then

$$K \sim T^{13/2-2m}, \tag{3.9}$$

which is constant for $m = 13/4 = 3.25$. This is gives a reasonable representation of the stratification of stars in convectively stable regions. At the bottom of the solar convection zone the density is about $200\,{\rm kg\,m^{-3}}$ and the temperature is about $2\times10^6\,{\rm K}$. This gives $K = (3-100)\times10^9\,{\rm kg\,m\,s^{-3}\,K^{-1}}$. In order to carry the solar flux the average temperature gradient then has to be around $0.01\,{\rm K/\,m}$.

However, in reality K changes slowly with height. Therefore the polytropic index effectively changes with height. In the outer layers the temperature decreases and there is ionisation and recombination. In that layer there are many electrons allowing for the formation of negative hydrogen ions, $\rm H^-$, from polarised neutral hydrogen atoms. This leads to low values of K. To transport the required energy flux, the temperature gradient has to go up. But this means the polytropic index goes down, see Eq. (2.53), and so the stratification will become unstable. This leads to convection in the outer parts of the Sun.

To a first approximation we can assume that convection leads to perfect mixing and therefore to a nearly uniform entropy distribution, corresponding to a state of marginal convective stability; see § 2.3.4. The star's stratification can then locally be described by a polytrope with $m = 3/2$ (for $\gamma = 5/3$). A plot of the resulting stratification is shown in Figure 3.1. However,

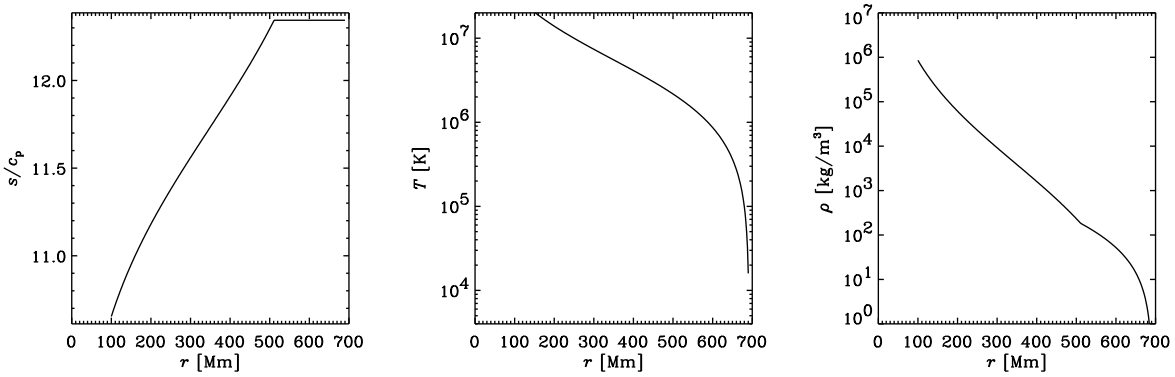

Figure 3.1: Simple polytropic stratification. The temperature is assumed to be inversely proportional to the conductivity, $K(z)$, such that $K\boldsymbol{\nabla}T = F_{\rm tot} = L/(4\pi r^2)$.

towards the surface layers cooling by radiation begins to play a role which causes the entropy to decrease gradually. A better approximation for the vertical stratification of density and temperature can be obtained by the mixing length theory, which will be discussed next. However, for more accurate and more detailed models one has to use numerical simulations, which are now beginning to become feasible.

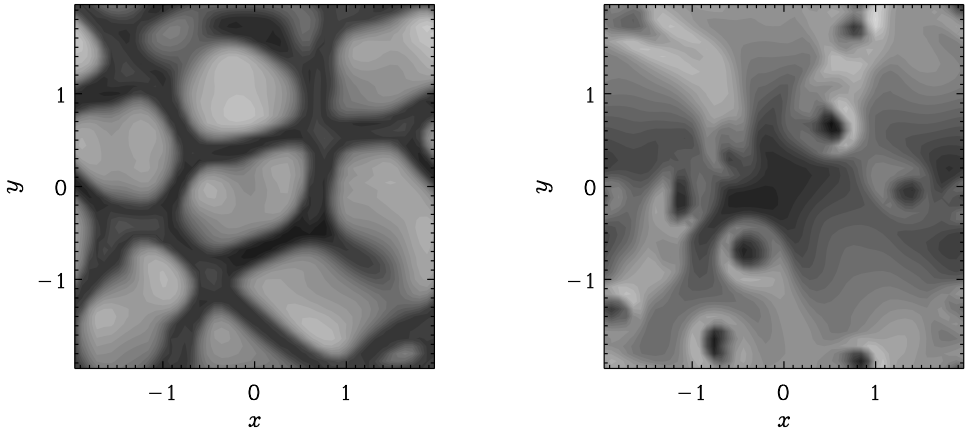

Figure 3.2: Images of temperature in surface and deeper layers of a convection simulation. Dark means lower temperatures and light higher temperatures.

3.3 Mixing length theory

3.3.1 Starting equations

- Buoyancy is balanced against advection, so $F_{\rm buoy} = F_{\rm D}^{\rm (turb)}$ and therefore $\Delta\varrho\, gV = C_{\rm D}\varrho v^2 S$, where V is the volume of the bubble and S is cross-sectional area. Denoting by $\ell \equiv V/(C_{\rm D}S)$ the mixing length, we have

$$v^2 = \frac{\Delta T}{T}\, g\ell. \tag{3.10}$$

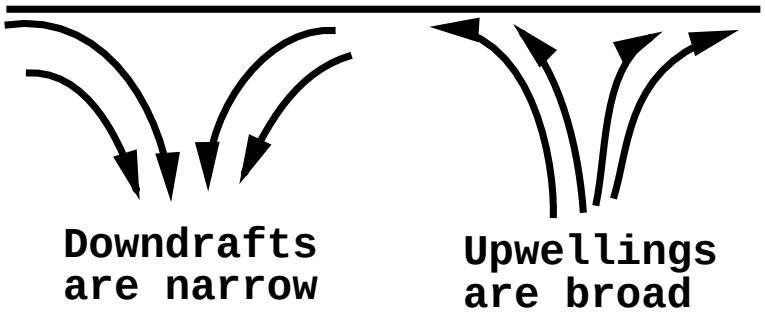

Figure 3.3: Downdrafts contract as they dive into deeper layers where the density is higher. On the other hand, upwellings expand as they ascend into the upper layers where the density is low.

- The only natural length scale in the problem is the scale height, so we assume that the mixing length is some fraction α of the local vertical pressure scale height, ie

$$\ell = \alpha H_p. \tag{3.11}$$

- The definition of the scale height is

$$H_p = \frac{\mathcal{R}T}{\mu g} = \frac{c_{\rm s}^2}{g}. \tag{3.12}$$

- The definition of the convective flux is

$$F_{\rm conv} = \varrho v c_p \Delta T. \tag{3.13}$$

  This expression shows that there is a positive convective flux if both the velocity is positive (upwards) and the temperature fluctuation is positive, ie if the upward moving fluid parcel is indeed warmer than its surroundings.

- There is actually a second expression for the convective flux, which is however more an approximation than a definition. We know convection can only occur when there is a downward entropy gradient, ie if the entropy decreases upwards. The entropy transport is stronger if the downward entropy gradient is stronger. To a first approximation the two are proportional to each other, ie

$$\mathbf{F}_{\rm conv} = -\chi_{\rm t} \varrho T \boldsymbol{\nabla} s \quad \text{if} \quad \mathbf{g} \cdot \boldsymbol{\nabla} s > 0, \tag{3.14}$$

  where $\chi_{\rm t}$ is a (turbulent) diffusion coefficient, and the ϱ and T factors have to be there on dimensional grounds.

- Like with all other types of diffusion coefficients, they are proportional to the speed of the fluid parcels accomplishing the diffusion, as well as the length over which such parcels stay coherent. Thus, we have

$$\chi_{\rm t} = c_\chi v \ell, \tag{3.15}$$

  where c_χ is another free parameter of order unity. (The other free parameter was α.)

This is the set of equations that we need to calculate the stratification in a convection zone. Some of the expressions above, especially (3.10), are severe approximations, and so one usually allows for extra non-dimensional factors in some of those expressions. This is why in other text books some of the expressions may involve somewhat different coefficients in places.

3.3.2 The entropy gradient

To calculate the stratification, the simplest approach was to assume that there was no entropy gradient at all within the convection zone (perfect mixing). With the equations derived above we can do better than that. The main thing we see from those equations is that v is proportional to $(\Delta T/T)^{1/2}$, see Eq. (3.10), and that therefore $F_{\rm conv}$ is proportional to $(\Delta T/T)^{3/2}$, see Eq. (3.13). Therefore,

$$\Delta T/T \sim F_{\rm conv}^{2/3} \quad \text{and} \quad v/c_{\rm s} \sim F_{\rm conv}^{1/3}. \tag{3.16}$$

Using Eq. (3.14) and the fact that $\chi_{\rm t} \sim v \sim F_{\rm conv}^{1/3}$ we have

$$F_{\rm conv} \sim F_{\rm conv}^{1/3} |ds/dz|, \tag{3.17}$$

or

$$|ds/dz| \sim F_{\rm conv}^{2/3}. \tag{3.18}$$

A proper calculation using the equations above shows that

$$\mathbf{g} \cdot \boldsymbol{\nabla} s/c_p = k \left(\frac{g}{c_{\rm s}}\right)^2 \left(\frac{F_{\rm conv}}{\varrho c_{\rm s}^3}\right)^{2/3} \tag{3.19}$$

where

$$k = \left(\frac{\gamma-1}{\gamma}\right)^{2/3} c_\chi^{-1} \alpha^{-4/3}, \tag{3.20}$$

which is around unity for $c_\chi = 1/3$ and $\alpha = 1.5$.

3.3.3 Calculating the stratification

If we assume that *all* the flux is carried by convection, ie if $F_{\rm tot} = F_{\rm conv}$, then we just have the following system of equations governing the stratification:

$$\frac{ds/c_p}{dz} = -\frac{g}{c_{\rm s}^2} k \left(\frac{F_{\rm tot}}{\varrho c_{\rm s}^3}\right)^{2/3}, \tag{3.21}$$

$$\frac{dp}{dz} = -\frac{g}{c_{\rm s}^2}, \tag{3.22}$$

together with $\ln \varrho = \frac{1}{\gamma} \ln p - s/c_p$, and $c_{\rm s}^2 = p/\varrho$. A solution of those equations is given in Figure 3.4. Note the almost perfectly flat s-gradient within the convection zone.

3.3.4 Including the radiative flux consistently

If the radiative flux is to be included consistently we have

$$F_{\rm rad} + F_{\rm conv} = F_{\rm tot}. \tag{3.23}$$

The radiative flux is

$$F_{\rm rad} = -K\frac{dT}{dz} = -KT\frac{d\ln T}{dz} = -KT\frac{d\ln p}{dz}\frac{d\ln T}{d\ln p}. \tag{3.24}$$

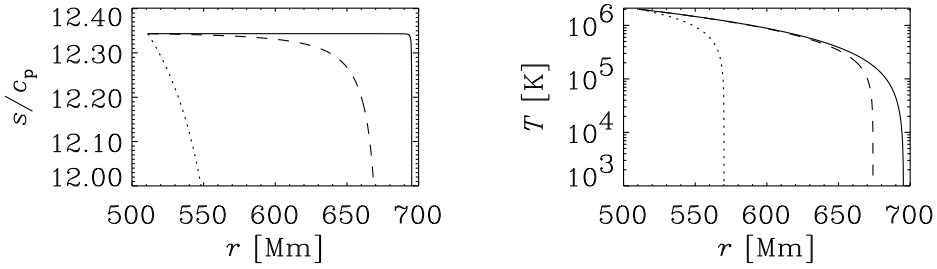

Figure 3.4: Mixing length stratification. The solid line is for solar luminosity, whilst the dashed and dotted lines are respectively for 10^6 and 10^9 times the solar value.

Here, $d\ln p/dz = -g/c_{\rm s}^2$, and $T = c_{\rm s}^2/(\mathcal{R}/\mu)$, so $c_{\rm s}^2$ cancels out and so

$$F_{\rm rad} = \frac{Kg}{\mathcal{R}/\mu}\,\frac{d\ln T}{d\ln p} \tag{3.25}$$

This can be expressed in terms of the entropy gradient using the differentiated form of Eq. (2.36),

$$ds/c_p = \frac{1}{\gamma} d\ln p - d\ln\varrho \tag{3.26}$$

which leads to

$$F_{\rm rad} = \frac{Kg}{\mathcal{R}/\mu}\left[\left(1-\frac{1}{\gamma}\right) + \frac{ds/c_p}{d\ln p}\right]. \tag{3.27}$$

Thus, the radiative flux has two contributions, one from the adiabatic temperature gradient (see **??**), and one from the super-adiabatic temperature gradient, so

$$F_{\rm rad} = F_{\rm rad}^{\rm (ad)} + K_r\,\frac{ds/c_p}{d\ln p}, \tag{3.28}$$

where

$$K_r = \frac{Kg}{\mathcal{R}/\mu} \quad \text{and} \quad F_{\rm rad}^{\rm (ad)} = K_r\left(\frac{\gamma-1}{\gamma}\right). \tag{3.29}$$

Inserting this into Eq. (3.23) we have

$$F_{\rm rad}^{\rm (ad)} + K_r\,\frac{ds/c_p}{d\ln p} + K_c\left(\frac{ds/c_p}{d\ln p}\right)^{3/2} = F_{\rm tot}, \tag{3.30}$$

where $K_c = \varrho c_{\rm s}^3/k^{3/2}$. We now introduce the additional abbreviations

$$\mathcal{G} \equiv \frac{ds/c_p}{d\ln p}, \quad \mathcal{F} \equiv \frac{F_{\rm tot} - F_{\rm rad}^{\rm (ad)}}{K_c}, \quad q = K_r/K_c, \tag{3.31}$$

so we can write

$$\mathcal{G}^{3/2} = q\mathcal{G} + \mathcal{F}, \tag{3.32}$$

which leads to a cubic equation for the entropy gradient, $\mathcal{G}$,

$$\mathcal{G}^3 - q^2\mathcal{G}^2 - 2q\mathcal{F}\mathcal{G} - \mathcal{F}^2 = 0. \tag{3.33}$$

A table of some values is given below, where we compare with the gradient, $\mathcal{G}_0 = (F_{\rm tot}/K_c)^{2/3}$, which is obtained when the radiative flux is neglected. An excellent approximation is to neglect q, in which case $\mathcal{G} = \mathcal{F}^{2/3}$, which is also given in the table.

Table 3.1: Solutions of the cubic equation for a solar model

r [Mm]	$T[10^6\,\mathrm{K}]$	$\mathcal{G}/10^{-6}$	$\mathcal{G}_0/10^{-6}$	$\mathcal{F}/10^{-9}$	$\mathcal{F}^{2/3}/10^{-6}$	$q/10^{-9}$
530	1.72	0.20	0.36	0.09	0.20	0.31
550	1.45	0.36	0.47	0.22	0.36	0.26
570	1.21	0.58	0.65	0.44	0.58	0.22
590	0.98	0.90	0.95	0.85	0.90	0.19
610	0.76	1.45	1.49	1.75	1.45	0.15
630	0.56	2.60	2.62	4.19	2.60	0.12
650	0.38	5.65	5.66	13.44	5.65	0.10
670	0.20	19.43	19.44	85.67	19.42	0.07
690	0.03	720.24	720.21	19329.29	719.98	0.02

3.4 Convective overshoot

Both numerical calculations of solar mixing length models as well as helioseismology (described below) indicate that the depth of the convection zone is about 200 Mm. However, near and beyond the boundaries of the convection zones the approximation (3.10) becomes very bad, because it ignores the fact that convective elements have inertia and can therefore overshoot a significant distance into the stably stratified regions. In those layers where the entropy gradient has reversed, a downward moving fluid parcel becomes hotter than its surroundings. Thus, in those layers the convection carries convective flux downwards, so its sign is reversed. This is shown in Figure 3.5 where profiles of entropy and convective flux, (3.13), are shown from a three-dimensional convection simulation.

Because of strong stratification, convection will be highly inhomogeneous, with narrow downdrafts and broad upwellings. This leads to a characteristic (but irregular) pattern of convection; see Figure 3.2. A sketch showing how stratification causes upwellings to broaden and downdrafts to converge is given in Figure 3.3.

3.5 Helioseismology

3.5.1 Acoustic waves in the Sun

Since the beginning of the eighties, standing acoustic waves in the Sun have been used to gain information about the interior of the Sun. It was possible to measure directly (ie without the use of any solar model)

- the radial dependence of the sound speed — and hence temperature

as well as

- the radial and latitudinal dependence of the internal angular velocity of the Sun.

This technique is called *helioseismology*, because it is mathematically similar to the techniques used in seismology of the Earth. Qualitatively, the radial dependence of the sound speed can be measured, because standing sound waves of different horizontal wave number penetrate to different depths. Therefore, the frequencies of those different waves depend on how exactly the sound speed changes with depth. Since the Sun rotates, the waves that travel in the direction

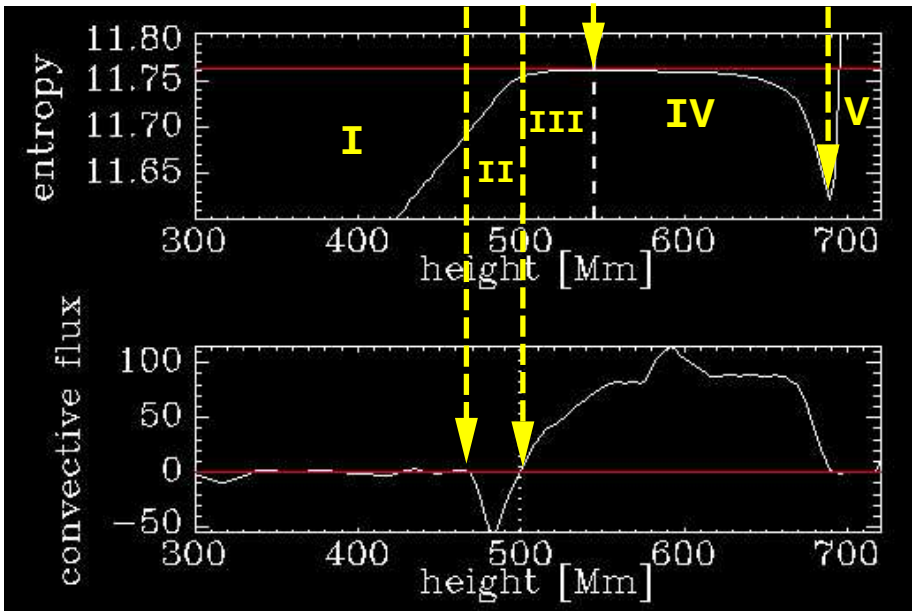

Figure 3.5: Profiles of entropy and convective flux. Region I is the radiative interior, II the overshoot layer, III the radiative heating layer, IV the bulk of the convection zone, and V the surface layer.

of rotation will be blue-shifted, and those that travel against the direction of rotation will be red-shifted. Therefore, the frequencies are split, depending on the amount of rotation in different layers.

Figure 3.6 shows the spatial pattern of a standing wave in three dimensions. It is the frequencies belonging to different latitudinal wave patterns that allow us to determine the latitudinal dependence of the angular velocity as well.

These acoustic waves are possible, because they are constantly being excited by the "noise" generated in the convection zone. The random fluctuations in the convection are turbulent and contain noise at all frequencies, similar to the noise generated by a glider going through the air. Now the Sun is a harmonic oscillator for sound waves and the different sound modes can be excited stochastically. This is similar to a bell in a sand storm starting to ring.

Figure 3.7 gives the result an inversion procedure that computes the radial dependence of the sound speed on depth, using the different frequency modes as input.

Helioseismology is a growing discipline, and more accurate data have now emerged due to the SOHO satellite and the GONG project (GONG = Global Oscillation Network Group), which has six stations around the globe to eliminate nightly gaps in the data.

3.5.2 Inverting the frequency spectrum

Like with a violin string, the acoustic frequency of the wave increases as the wavelength decreases, ie

$$\text{frequency} \propto 1/\text{wavelength}. \tag{3.34}$$

More precisely, the frequency ω is given by

$$\omega = c_{\rm s} k, \tag{3.35}$$

where $c_{\rm s}$ is the sound speed and $k = 2\pi/\lambda$ is the wavenumber (λ is the wavelength). If sound waves travel an oblique path then we can express the wavenumber in terms of its horizontal

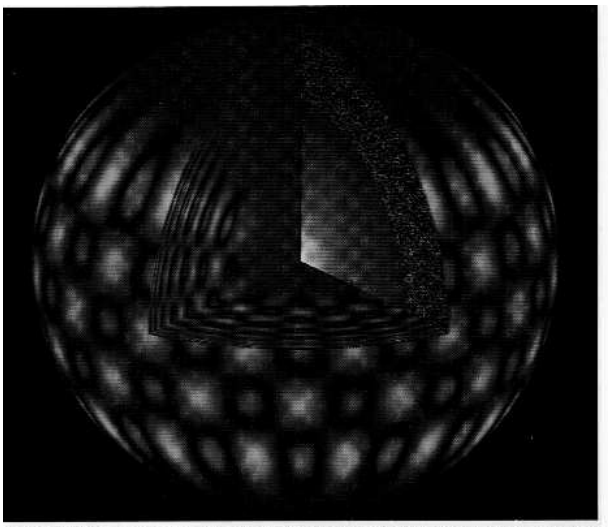

IGURE 13.18 Computer model of some of the resonant tones of the solar interior. Blue epresents expanding regions; red, contracting ones. The pattern on the photosphere esults from the resonances of waves in the sun's interior. The patterned region just elow the surface represents the sun's convection zone. (Courtesy of NOAO.)

Figure 3.6: Three-dimensional wave pattern of a single wave mode. In reality, millions of different wave patterns are all superimposed.

and vertical wave numbers, $k_{\rm h}$ and $k_{\rm v}$, respectively. We do this because only the horizontal wavenumber can be observed. This corresponds to the horizontal pattern in Figure 3.6. Thus, we have

$$k^2 = k_{\rm h}^2 + k_{\rm v}^2 \ . \tag{3.36}$$

The number of radial nodes of the wave is given by the number of waves that fit into the Sun, or at least the part of the Sun where the corresponding wave can travel. This part of the Sun will be referred to as cavity. The larger the cavity is, the more nodes there will be for a given wavelength. The number of modes n is then given by

$$n = 2\Delta r/\lambda = 2\Delta r \frac{k_{\rm v}}{2\pi} = \Delta r\, k_{\rm v}/\pi \ , \tag{3.37}$$

where Δr is the radial extent of the cavity. If the sound velocity and, hence, $k_{\rm v}$ depends on radius, this formula must be generalised to

$$n = \frac{1}{\pi} \int_{r_{\rm min}}^{R_\odot} k_{\rm v}\, dr, \tag{3.38}$$

supposing the cavity to be the spherical shell $r_{\rm min} < r < R_\odot$.

The horizontal pattern of the proper oscillation is described by spherical harmonics with indices l and m, hence the horizontal wave number is

$$k_{\rm h}^2 = \frac{l(l+1)}{r^2} \tag{3.39}$$

and we can write

$$k_{\rm v} = \sqrt{\frac{\omega^2}{c_{\rm s}^2} - \frac{l(l+1)}{r^2}} = \frac{\omega}{r}\sqrt{\frac{r^2}{c_{\rm s}^2} - \frac{l(l+1)}{\omega^2}} \tag{3.40}$$

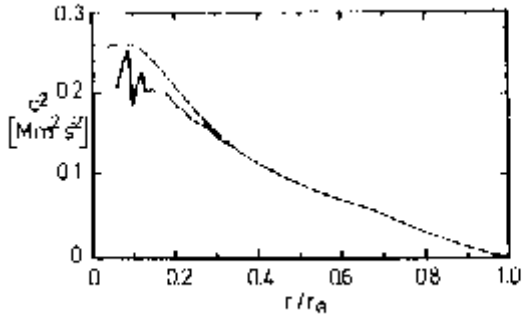

Fig. 5.18. Square of the sound speed in the Sun. *Continuous line:* inversion of the data in Fig. 5.15; *dashed:* theoretical solar model. From Christensen-Dalsgaard et al. (1985)

Figure 3.7: Radial dependence of the sound speed on radius in the Sun. Note the change in slope near $r = 0.7$ solar radii. The oscillations near the centre are not physical. The theoretical model (dotted line) is in fair agreement with the direct measurements. The sound speed has its maximum not in the centre, because the mean molecular weight μ increases towards the centre, which causes c_s to decrease. (Note that $c_\mathrm{s}^2 = \mathcal{R}T/\mu$.)

Therefore, the number n of radial nodes is given by

$$\frac{\pi(n+\alpha)}{\omega} = \int_{r_\mathrm{min}}^{R_\odot} \sqrt{\frac{r^2}{c_\mathrm{s}^2} - \frac{l(l+1)}{\omega^2}}\,\frac{dr}{r}. \tag{3.41}$$

The phase shift $\alpha \approx 1.5$ accounts for the fact that the standing waves are confined by "soft" and extended, rather than fixed, boundaries.

Introducing new variables

$$\xi \equiv \frac{r^2}{c_\mathrm{s}^2}, \qquad u \equiv \frac{l(l+1)}{\omega^2} \tag{3.42}$$

and denoting the left hand side by $F(u)$, we can write

$$F(u) = \int_u^{\xi_\odot} \sqrt{\xi - u}\,\frac{d\ln r}{d\xi}\,d\xi. \tag{3.43}$$

Since we know, at least in principle, $F(u)$ from observations and are interested in the connection between r and ξ (i.e. r and c_s), we interpret (3.43) as an integral equation for the unknown function $r(\xi)$.

Most integral equations cannot be solved in closed form, but this one can. Differentiate (3.43) with respect to u and, in the final result, rename ξ to ξ':

$$\frac{dF}{du} \equiv F'(u) = -\frac{1}{2}\int_u^{\xi_\odot} \frac{1}{\sqrt{\xi - u}}\,\frac{d\ln r}{d\xi}\,d\xi - 1\cdot\sqrt{u-u}\,\left.\frac{d\ln r}{d\xi}\right|_{\xi=u}, \tag{3.44}$$

i.e.

$$F'(u) = -\frac{1}{2}\int_u^{\xi_\odot} \frac{1}{\sqrt{\xi' - u}}\,\frac{d\ln r}{d\xi'}\,d\xi'. \tag{3.45}$$

This is Abel's integral equation. It can be solved analytically: Multiply by $1/\sqrt{u-\xi}$ and integrate from $u=\xi$ to $u=\xi_\odot$.

$$\int_\xi^{\xi_\odot} \frac{F'(u)}{\sqrt{u-\xi}}\,du = -\frac{1}{2}\int_\xi^{\xi_\odot} du\,\frac{1}{\sqrt{u-\xi}}\int_u^{\xi_\odot} d\xi'\frac{1}{\sqrt{\xi'-u}}\frac{d\ln r}{d\xi'} = -\frac{1}{2}\int_\xi^{\xi_\odot} du\int_u^{\xi_\odot} d\xi'\,\frac{1}{\sqrt{(u-\xi)(\xi'-u)}}\frac{d\ln r}{d\xi'} \tag{3.46}$$

Due to the unknown function $\ln r(\xi')$, we cannot explicitly carry out the integration with respect to ξ', but integrating over u will be possible. In order to do this, we interchange the order of integration.

Interchanging the order of integration: This would be easy if integration were over a rectangular region. In our case, where the integration bounds for ξ' depend on u, the graphical representation on the right shows us what to do.
We can *either* let u run from ξ to $\xi_\odot$ (the outer integral) and for every given u integrate over ξ' from $\xi'=u$ to $\xi'=\xi_\odot$ (the inner integral).
Or we can choose the outer integration to be over ξ' from $\xi'=\xi$ to $\xi'=\xi_\odot$ and for every given value of ξ' integrate over u from $u=\xi$ to $u=\xi'$.
Hence,

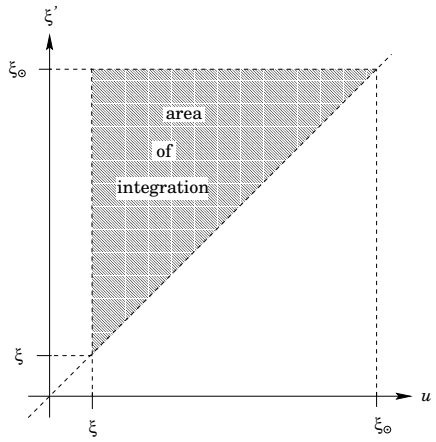

$$\int_\xi^{\xi_\odot} du\int_u^{\xi_\odot} d\xi'(\dots) = \int_\xi^{\xi_\odot} d\xi'\int_\xi^{\xi'} du(\dots), \tag{3.47}$$

where $(\dots)$ stands for an arbitrary integrand.

With this, (3.46) becomes

$$\int_\xi^{\xi_\odot} \frac{F'(u)}{\sqrt{u-\xi}}\,du = -\frac{1}{2}\int_\xi^{\xi_\odot} d\xi'\,\frac{d\ln r}{d\xi'}\int_\xi^{\xi'} \frac{du}{\sqrt{(u-\xi)(\xi'-u)}} \tag{3.48}$$

The integral over u can now be evaluated analytically. One way to do this involves a trigonometric substitution of variables. Alternatively, we can have a close look at the integrand, which is sketched in Figure 3.8.

The integrand $f(u)$ is symmetric with respect to $(\xi'+\xi)/2$, which motivates introduction of a new integration variable v in the following way:

$$u = \frac{\xi'+\xi}{2} + \frac{\xi'-\xi}{2}v \tag{3.49}$$

with

$$du = \frac{\xi'-\xi}{2}\,dv, \qquad u-\xi = \frac{\xi'-\xi}{2}\,(1+v), \qquad \xi'-u = \frac{\xi'-\xi}{2}\,(1-v), \tag{3.50}$$

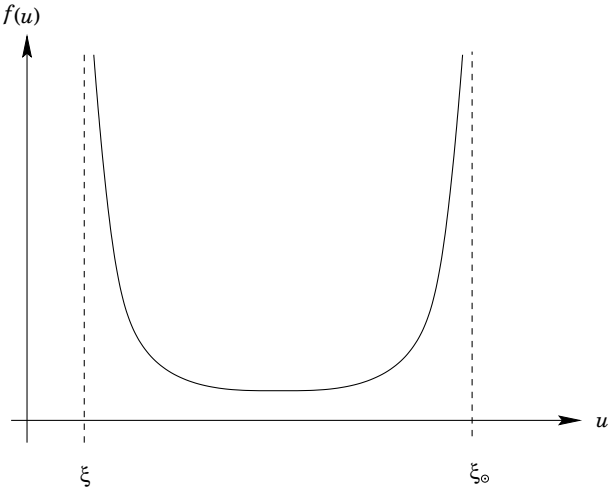

Figure 3.8: Sketch of the integrand $f(u) \equiv \dfrac{1}{\sqrt{(u-\xi)(\xi'-u)}}$ as a function of u.

Obviously, $u = \xi$ corresponds to $v = -1$, while $u = \xi'$ for $v = 1$. Thus,

$$\int_{\xi}^{\xi'} \frac{du}{\sqrt{(u-\xi)(\xi'-u)}} = \int_{-1}^{1} \frac{\frac{\xi'-\xi}{2}}{\sqrt{(\frac{\xi'-\xi}{2})^2(1-v^2)}}\, dv = \int_{-1}^{1} \frac{dv}{\sqrt{1-v^2}} = \arcsin v \Big|_{-1}^{1} = \frac{\pi}{2} - (-\frac{\pi}{2}) = \pi \tag{3.51}$$

Inserting this into (3.46), we obtain

$$\int_{\xi}^{\xi_\odot} \frac{F'(u)}{\sqrt{u-\xi}}\, du = -\frac{\pi}{2} \int_{\xi}^{\xi_\odot} \frac{d\ln r}{d\xi'}\, d\xi' = -\frac{\pi}{2}\, \ln r \Big|_{\xi'=\xi}^{\xi_\odot} = \frac{\pi}{2} \ln \frac{r(\xi)}{R_\odot} \tag{3.52}$$

We can solve this equation for $r(\xi)$:

$$r(\xi) = R_\odot \exp\left(\frac{2}{\pi} \int_{\xi}^{\xi_\odot} \frac{F'(u)}{\sqrt{u-\xi}}\, du \right) \tag{3.53}$$

This is the final result of inverting the integral equation (3.43). It establishes the link we were looking for between the observable function $F(u)$ and the function $r(\xi)$, from which the radial profile of the sound velocity c_s can directly be obtained.

Chapter 4

Magnetic fields

This chapter contains more material than will be presented in the course. The extra material is included mainly for interest.

4.1 The Lorentz force

Astrophysical bodies are almost always electrically conducting and can thus interact with magnetic fields. The first example concerns the support of prominences against gravity by a magnetic field. We have dealt with the effect of magnetic fields on charged particles already in § 2.1.1. There, we considered only one particle and the force exerted on a single particle was given by $q\mathbf{v}\times\mathbf{B}$. Now, if there are many particles with given number density n (= number of particles per unit volume), then the force on the gas per unit volume will be $nq\mathbf{v}\times\mathbf{B}$. The expression $nq\mathbf{v}$ is the current density, so

$$\mathbf{J}\equiv nq\mathbf{v}. \tag{4.1}$$

Thus the Lorentz force per unit volume is $\mathbf{J}\times\mathbf{B}$ and, if there are no other terms, this will accelerate the gas. The acceleration per unit volume is $\varrho d\mathbf{v}/dt$, so the equation of motion takes the form

$$\varrho\frac{d\mathbf{v}}{dt}=\mathbf{J}\times\mathbf{B}+\text{possibly further terms.} \tag{4.2}$$

In order to calculate this force, we have to express $\mathbf{J}$ in terms of other known quantities. At this point we may express $\mathbf{J}$ using one of Maxwell's equations

$$\mu_0\mathbf{J}=\boldsymbol{\nabla}\times\mathbf{B}, \tag{4.3}$$

which is also called Ampère's law, and where the Faraday displacement current $c^{-2}\partial\mathbf{E}/\partial t$ is neglected. Thus the Lorentz force takes the form $\mathbf{F}_L\equiv\mathbf{J}\times\mathbf{B}=\frac{1}{\mu_0}(\boldsymbol{\nabla}\times\mathbf{B})\times\mathbf{B}$, which can also be written in the form

$$\mathbf{F}_L=-\boldsymbol{\nabla}(\mathbf{B}^2/2\mu_0)+(\mathbf{B}\cdot\boldsymbol{\nabla})\mathbf{B}/\mu_0, \tag{4.4}$$

which shows that the Lorentz force has a gradient term (magnetic pressure gradient) and a derivative of the field strength along the direction of the field. The latter tends to contract field lines (magnetic tension).

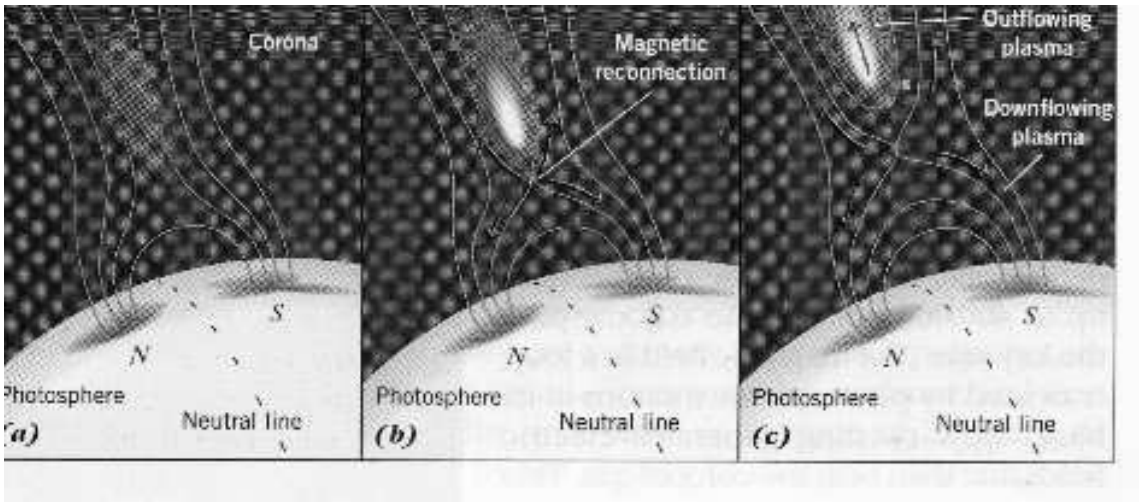

Figure 4.1: Magnetic support of a flare.

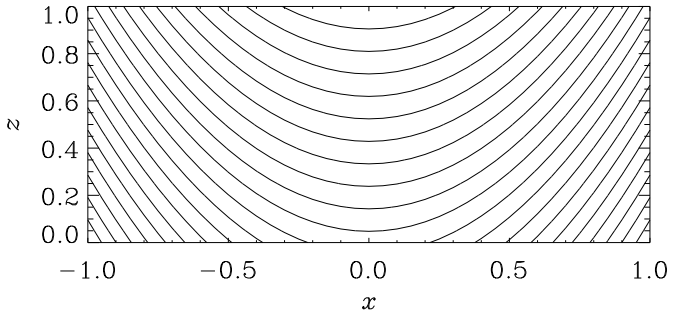

Figure 4.2: Contours of $A = z - x^2$, as a model for magnetic field lines supporting prominences against gravity.

4.2 Magnetic support of prominences

The magnetic field is able to support fluid against gravity. An example is the quasi-steady support of prominences in the solar corona. Figure 4.1 shows a simple cartoon picture of a V-shaped magnetic field line where the Lorentz force points upwards, trying to move fluid with the field lines such as to shorten the field lines.

We take a simple parabola-shaped field line. In order to automatically satisfy the condition $\boldsymbol{\nabla} \cdot \mathbf{B} = 0$ we write $\mathbf{B} = \boldsymbol{\nabla} \times (A\hat{\mathbf{y}})$, where $\hat{\mathbf{y}}$ is the unit vector in the direction out of the paper. The lines $A = \text{const}$ are parallel to field lines (at least in two dimensions). This can be verified by showing that the gradient of A is perpendicular to $\mathbf{B}$:

$$\mathbf{B} \cdot (\boldsymbol{\nabla} A) = \begin{pmatrix} -\partial_z A \\ 0 \\ \partial_x A \end{pmatrix} \cdot \begin{pmatrix} \partial_x A \\ 0 \\ \partial_z A \end{pmatrix} = 0. \tag{4.5}$$

Now, we write our parabola-shaped field lines as

$$A = z - x^2, \tag{4.6}$$

see Figure 4.2. Let us now calculate the resulting field, current and Lorentz force:

$$\mathbf{B} = \begin{pmatrix} \partial_x \\ 0 \\ \partial_z \end{pmatrix} \times \begin{pmatrix} 0 \\ z - x^2 \\ 0 \end{pmatrix} = \begin{pmatrix} -1 \\ 0 \\ -2x \end{pmatrix} \tag{4.7}$$

Thus, the current is then

$$\mathbf{J} = \frac{1}{\mu_0} \begin{pmatrix} \partial_x \\ 0 \\ \partial_z \end{pmatrix} \times \begin{pmatrix} -1 \\ 0 \\ -2x \end{pmatrix} = \frac{1}{\mu_0} \begin{pmatrix} 0 \\ 2 \\ 0 \end{pmatrix}, \tag{4.8}$$

and so the Lorentz force is

$$\mathbf{J} \times \mathbf{B} = \frac{1}{\mu_0} \begin{pmatrix} 0 \\ 2 \\ 0 \end{pmatrix} \times \begin{pmatrix} -1 \\ 0 \\ -2x \end{pmatrix} = \frac{1}{\mu_0} \begin{pmatrix} -4x \\ 0 \\ 2 \end{pmatrix}, \tag{4.9}$$

ie the Lorentz force has a vertical component upwards and points towards the z-axis.

4.3 Magnetic field evolution

The evolution of the magnetic field is governed by the Faraday equation

$$\frac{\partial \mathbf{B}}{\partial t} = -\boldsymbol{\nabla} \times \mathbf{E}, \tag{4.10}$$

Ampère's equation

$$\mathbf{J} = \boldsymbol{\nabla} \times \mathbf{B}/\mu_0, \tag{4.11}$$

and Ohm's law,

$$\mathbf{J} = \sigma(\mathbf{E} + \mathbf{v} \times \mathbf{B}). \tag{4.12}$$

Eliminating $\mathbf{E}$ using (4.10) and (4.12) we obtain the induction equation,

$$\frac{\partial \mathbf{B}}{\partial t} = \boldsymbol{\nabla} \times (\mathbf{v} \times \mathbf{B} - \mathbf{J}/\sigma). \tag{4.13}$$

The quantity σ is here the conductivity (not to be confused with the Stefan-Boltzmann constant!!). The magnetic diffusivity is $\eta = (\mu_0 \sigma)^{-1}$ and has dimensions m^2/s. If η is constant, then the induction equation can also be written in the form

$$\frac{\partial \mathbf{B}}{\partial t} = \boldsymbol{\nabla} \times (\mathbf{v} \times \mathbf{B}) + \eta \nabla^2 \mathbf{B}. \tag{4.14}$$

In SI units Maxwell's equations can be written in the form

$$\frac{\partial \mathbf{B}}{\partial t} = -\boldsymbol{\nabla} \times \mathbf{E}, \quad \text{Faraday's law} \tag{4.15}$$

$$\mu_0 \mathbf{J} + \frac{1}{c^2}\frac{\partial \mathbf{E}}{\partial t} = \boldsymbol{\nabla} \times \mathbf{B}, \quad \text{Ampère's law} \tag{4.16}$$

together with

$$\boldsymbol{\nabla} \cdot \mathbf{B} = 0, \quad \text{and} \quad \boldsymbol{\nabla} \cdot \mathbf{E} = \varrho_e \tag{4.17}$$

where ϱ_e is the charge density. The $\partial \mathbf{E}/\partial t$ term is also called the Faraday displacement current. It is usually small compared with the other two terms in that equation. There are two exceptions where it can become important: (i) if there is a vacuum, ie if the ordinary current $\mathbf{J}$ vanishes, see Eq. (4.12), or if there are rapid variations over large length scales so that the Faraday displacement current becomes comparable to $\boldsymbol{\nabla} \times \mathbf{B}$, ie the typical velocity becomes comparable with the speed of light. The former occurs in the atmosphere, where it is responsible for radio waves, whilst the latter may become important near a black hole, where all velocities become comparable with the speed of light. In all other cases the Faraday displacement current may safely be neglected. The resulting equations are also called the pre-Maxwell equations.

4.4 Frozen-in magnetic fields

If magnetic diffusion vanishes, ie $\eta \to 0$ and $\sigma \to \infty$ (high conductivity limit), we may neglect the diffusion term and the induction equation then takes the form

$$\frac{\partial \mathbf{B}}{\partial t} = \boldsymbol{\nabla} \times (\mathbf{v} \times \mathbf{B}) = -(\mathbf{v} \cdot \boldsymbol{\nabla})\mathbf{B} + (\mathbf{B} \cdot \boldsymbol{\nabla})\mathbf{v} - \mathbf{B}(\boldsymbol{\nabla} \cdot \mathbf{v}). \tag{4.18}$$

Compare this now with the evolution equation of a material line element, $\delta \mathbf{l}$. Let $\mathbf{v}$ be the velocity on one end of the line element, then the velocity at the other end of the line element $\delta \mathbf{l}$ is $\mathbf{v} + (\delta \mathbf{l} \cdot \boldsymbol{\nabla})\mathbf{v}$. Thus, within the time dt the change of $\delta \mathbf{l}$ is equal to $dt \delta \mathbf{l}$. Therefore the evolution of $\delta \mathbf{l}$ satisfies the equation

$$\frac{d}{dt}\delta \mathbf{l} = (\delta \mathbf{l} \cdot \boldsymbol{\nabla})\mathbf{v} \tag{4.19}$$

This equation is equivalent to the evolution equation of the magnetic field if $\eta = 0$ and if $\boldsymbol{\nabla} \cdot \mathbf{v} = 0$ is assumed. The latter assumption is unessential: if $\boldsymbol{\nabla} \cdot \mathbf{v} \neq 0$ then we have to invoke the continuity equation

The derivative d/dt is here taken in a frame co-moving with the fluid at speed $\mathbf{v}$. This derivative is also called lagrangian derivative; to emphasise that one deals with a lagrangian derivative one often uses a capital D for the differential. Expressing it in terms of the normal non-moving frame of reference this becomes

$$D/Dt \equiv \partial/\partial t + (\mathbf{v} \cdot \boldsymbol{\nabla}). \tag{4.20}$$

If the velocity is divergence-free (no sources or sinks, ie the flow is incompressible) then the magnetic field evolves according to

$$\frac{D\mathbf{B}}{Dt} = (\mathbf{B}\cdot\boldsymbol{\nabla})\mathbf{v}, \tag{4.21}$$

which is exactly the same equation as that for $\delta\mathbf{l}$. Thus,we conclude that the magnetic field vectors evolve in the same way as material line elements do. If the $\mathbf{B}$-vectors had finite length, the two ends of the vector would coincide with the locations of particles in the flow. Furthermore, if the flow diverges locally it will stretch the magnetic field lines, which will leads to their enhancement. This stretching is an important ingredient of all dynamos.

4.5 The magnetic vector potential

It is sometimes convenient to consider the evolution of the vector potential $\mathbf{A}$, because then the magnetic field $\mathbf{B} = \boldsymbol{\nabla}\times\mathbf{A}$ is guaranteed to be divergence-free. The induction equation (4.13) can be "uncurled", ie the curl can be removed on both sides of the equation. However, this leads to an uncertainly, because a gradient term could always be added to the uncurled equation without changing $\mathbf{B}$. Thus, we have

$$\frac{\partial\mathbf{A}}{\partial t} = \mathbf{v}\times\mathbf{B} - \mathbf{J}/\sigma - \boldsymbol{\nabla}\phi, \tag{4.22}$$

where ϕ is called the gauge potential, which is really like an integration constant. We are free to choose any gauge that is convenient. Note that

$$\mu_0\mathbf{J} = \boldsymbol{\nabla}\times\boldsymbol{\nabla}\times\mathbf{A} \equiv -\nabla^2\mathbf{A} + \boldsymbol{\nabla}(\boldsymbol{\nabla}\cdot\mathbf{A}). \tag{4.23}$$

A convenient gauge is the so-called Lorentz gauge,

$$\phi = \boldsymbol{\nabla}\cdot\mathbf{A}, \tag{4.24}$$

in which the evolution equation for $\mathbf{A}$ becomes

$$\frac{\partial\mathbf{A}}{\partial t} = \mathbf{v}\times\mathbf{B} + \eta\nabla^2\mathbf{A}. \tag{4.25}$$

However, this works only if the magnetic diffusivity $\eta = (\mu_0\sigma)^{-1}$ is constant.

4.6 Flux conservation

The condition $\boldsymbol{\nabla}\cdot\mathbf{B} = 0$ means that there are no magnetic monopoles, from which magnetic field lines would originate. This becomes obvious when taking the volume integral of $\boldsymbol{\nabla}\cdot\mathbf{B} = 0$, which can be turned into a surface integral by Gauss' integral theorem; so

$$0 = \int_V \mathbf{B}\,dV = \oint_S \mathbf{B}\cdot d\mathbf{S}, \tag{4.26}$$

see Figure 4.3. Here, $S = \partial V$ is the closed surface bounding the volume V. If field lines go out of the volume, then there must be an equal amount of field lines going into the volume, such that $\oint_S \mathbf{B}\cdot d\mathbf{S} = 0$.

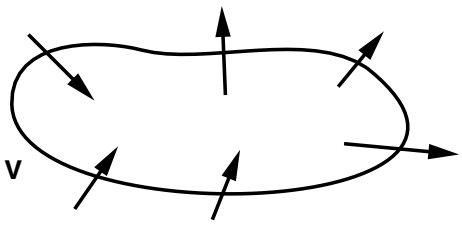

Figure 4.3: Flux conservation. As many field lines enter the volume as field lines leave the volume.

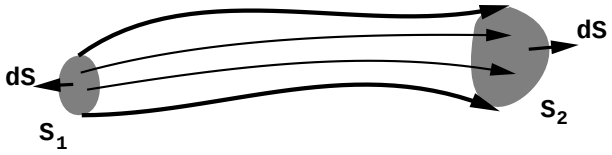

Figure 4.4: Flux conservation. The total surface integral gives zero: nothing comes from the wall of the tube and the contributions from the two ends must be equal in magnitude, but of opposite sign.

In Figure 4.4 we consider the magnetic field in a tube (flux tube). Only at the two ends does the field stick out of the tube. Integrating over the tube we have

$$0 = \oint_S \mathbf{B} \cdot d\mathbf{S} = \oint_{S_1} \mathbf{B} \cdot d\mathbf{S} + \oint_{S_2} \mathbf{B} \cdot d\mathbf{S}. \tag{4.27}$$

Note that in Figure 4.4 the normal of the surface element points outwards. We now define the flux though a surface S as

$$\Phi = \int_S \mathbf{B} \cdot d\mathbf{S}, \tag{4.28}$$

where now $d\mathbf{S}$ points always in the same direction. Then we see that

$$\Phi = \text{constant along the tube.} \tag{4.29}$$

This property is referred to as flux conservation.

4.7 Connection with topology

The dot product $\mathbf{A} \cdot \mathbf{B}$ is of some importance in that it can be related to the topology of magnetic flux ropes. Let us define the quantity

$$H = \int_V \mathbf{A} \cdot \mathbf{B}\, dV, \tag{4.30}$$

where the integration volume is chosen such that the normal component of $\boldsymbol{\mathcal{B}}$ vanishes on the boundary, ie $\hat{\mathbf{n}} \cdot \mathbf{B} = 0$. Let us consider two interlinked flux loops (Figure 4.5).

For the volume V_1 of the first loop we have

$$H_1 = \int_{V_1} \mathbf{A} \cdot \mathbf{B}\, dV = \int_{V_1} \mathbf{A} \cdot \mathbf{B}\, (d\mathbf{l} \cdot d\mathbf{S}), \tag{4.31}$$

where $d\mathbf{S}$ is the surface element across the tube and $d\mathbf{l}$ is the line element along the tube. Note that $\mathbf{B} \parallel d\mathbf{l} \parallel d\mathbf{S}$, so the integral can also be written as $\int (\mathbf{A} \cdot d\mathbf{l})(\mathbf{B} \cdot d\mathbf{S})$. In $\mathbf{A} \cdot \mathbf{B}$ only the

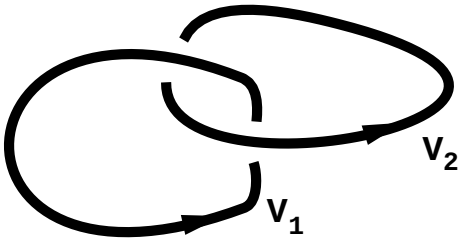

Figure 4.5: Two interlinked flux loops.

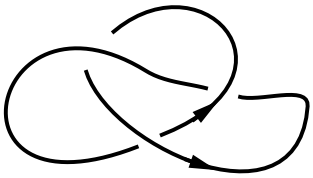

Figure 4.6: The trefoil knot.

component of $\mathbf{A}$ that is parallel to $\mathbf{B}$ (and $d\mathbf{l}$) matters. This component is only affected by the field of the other tube, but since the field of the other tube vanishes inside V_1, the parallel component of $\mathbf{A}$ must be *constant* in V_1. Therefore we can split the integral into two separate integrals, so

$$H_1 = \left(\int_{S_1} \mathbf{B} \cdot d\mathbf{S}\right) \left(\oint_{C_1} \mathbf{A} \cdot d\mathbf{l}\right), \tag{4.32}$$

where C_1 is a closed line along the tube. (It doesn't matter where across the tube this line goes because the parallel component of $\mathbf{A}$, and therefore also $\mathbf{A} \cdot d\mathbf{l}$, is constant). Now, the first integral is just the flux Φ_1 of the first tube. The second integral is actually the flux of the second tube, Φ_2, because, according to Stokes' integral theorem,

$$\Phi_2 = \int_{S_2} \mathbf{B} \cdot d\mathbf{S} = \int_{S(C_1)} (\boldsymbol{\nabla} \times \mathbf{B}) \cdot d\mathbf{S} = \oint_{C_1} \mathbf{A} \cdot d\mathbf{l}. \tag{4.33}$$

Here $S(C_1)$ is the surface enclosed by the curve C_1. We were able to take the integral over this bigger cross-section, because the field outside S_2 and inside $S(C_1)$ vanishes. Therefore,

$$H_1 = \Phi_1 \Phi_2. \tag{4.34}$$

By the same arguments we find the same result for H_2 when considering the other tube, so $H_2 = \Phi_1 \Phi_2$. Therefore the integral over all space is

$$H = \int_V \mathbf{A} \cdot \mathbf{B}\, dV = H_1 + H_2 = 2\Phi_1 \Phi_2. \tag{4.35}$$

For loops that are linked in more complicated ways one gets the product of the fluxes multiplied by the winding number. In particular, for the trefoil knot shown in Figure 4.6, one gets the result $H = 2\Phi^2$, even through this knot consists only of a single (knotted) flux tube.

Chapter 5

Accretion discs in binaries

We have already mentioned the formation of discs in connection with the planetary system. The same idea applies also to binary stars and to centres of galaxies. In the former case mass is being transferred from one component to the other either via a wind (in the case of a hot donor) or via Roche lobe overflow (see Figure 5.1).

In the second case, the centres of galaxies, the situation is even more reminiscent of planetary systems, but on a larger scale and with different temperatures involved. Both in the centres of galaxies as well as in protostellar discs one starts from a more-or-less homogeneous cloud that collapses, but because of rotation there will be a time during the collapse when the centrifugal force begins to balance gravity. This is the point when a disc is formed and further radial infall is only possible because there is either a viscous or a magnetic torque that removes angular momentum outwards.

In the following we consider the standard case of a viscous accretion disc with given viscosity. Because discs are thin it is possible to calculate the radial structure analytically. This thin-disc solution is due to Shakura & Sunyaev (1973) and it has become an important mile stone in modern astrophysics.

Before deriving the governing equations and the standard solution we first explain in qualitative terms how discs occur in binary systems.

5.1 Binary stars

More than 50% of the stars are binary stars. Some say the higher probability of finding binary stars is because they are counted twice. Anyway, binary stars can be divided into three different classes: detached, semi-detached, and contact binaries.

Detached binaries are relatively boring from a hydrodynamical view point, unless they are close enough to lead to tidal coupling between the two components, for example. However, detached binaries may evolve. The heavier of the two components will at some point develop into a red giant, which is so big that it will "fill its Roche-lobe". That means matter will start to flow to the other component. (We will take a closer look at the Roche potential and the dynamics of overflow in the course MAS371.) What is now crucial for us is the fact that the overflowing matter has angular momentum and will therefore be unable to fall onto the secondary star directly. This is why a disc is formed. We encountered a similar problem earlier in connection with star formation where, again, matter was unable to fall directly onto the central object because of rotation. Instead a disc was formed. Such discs are typically viscous in the sense that turbulence in them leads to friction which allows angular momentum to be removed, so matter can move in further towards the central object.

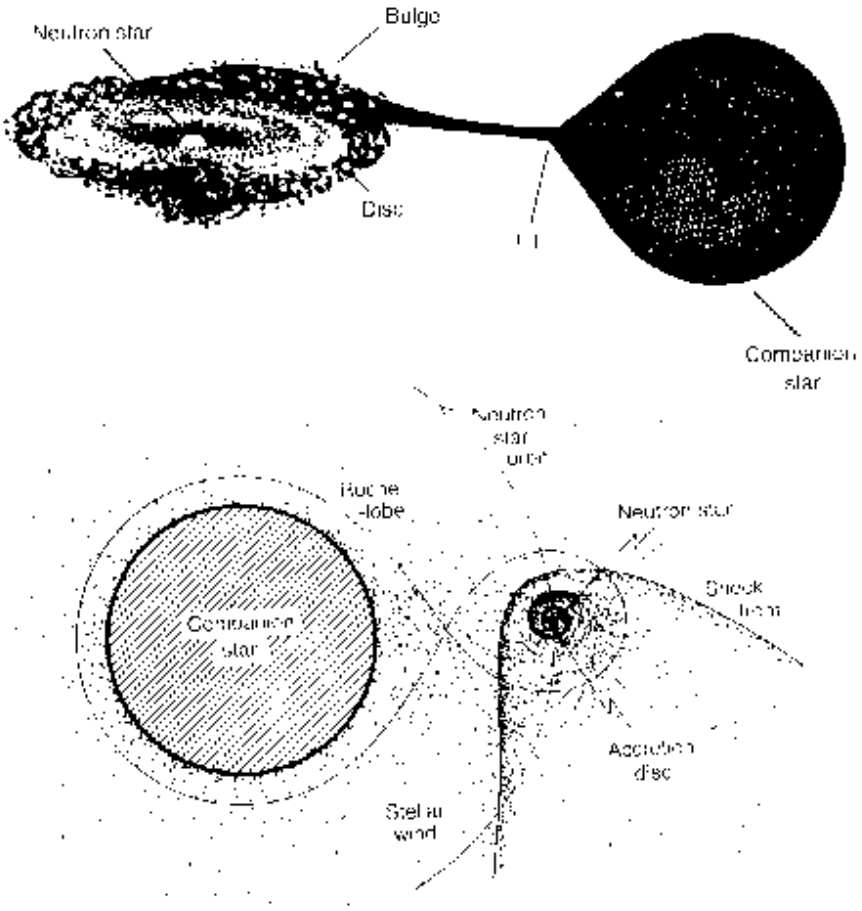

Figure 5.1: Accretion onto a companion star via Roche lobe overflow (upper panel) and via a wind (lower panel).

5.2 Accretion discs

In this section we explain the basic theory used to describe the radial structure of accretion discs. This theory is mathematically simple, because it involves only algebraic equations, and it is physically rather powerful, because complicated physical processes can be taken into account.

As we mentioned in the beginning, the theory is important because it is applicable to a wide range of different astrophysical bodies: protostellar and protoplanetary discs, discs in X-ray binaries and other binary systems, and discs in active galactic nuclei and centres of galaxies.

To obtain the governing equations we derive vertically integrated equations for the mechanical equilibrium in the vertical and horizontal directions, as well as the thermal equilibrium. An important quantity in this business is the vertically integrated density $\sigma \equiv \int_{-\infty}^{\infty} \varrho \, dz$, where H is the half thickness of the disc. However, no attempt is usually made to consider the vertical integration as an exact procedure. It is merely just a replacement of ϱ by its value in the central plane, ϱ_c, which is then replaced in all the equations by σ/H.

5.2.1 Vertical equilibrium

In § 2.6.3 we showed that the vertical component of gravity in a disc is

$$g_z = -\Omega^2 z. \tag{5.1}$$

As usual, this force has to be balanced by a pressure gradient, so in the steady state the vertical momentum equation becomes simply

$$0 = -\frac{\partial p}{\partial z} + \varrho g_z. \tag{5.2}$$

This can be integrated in certain cases, eg for the case of constant temperature or under the assumption of a polytropic atmosphere. However, the result is qualitatively always similar and only some numerical coefficients change.

A simple and instructive example is one where the density is constant (and equal to ϱ_c) within the disc, $|z| < H$, and zero outside, ie $|z| > H$. In that case Eq. (5.2) can be integrated as follows:

$$-\int_0^H \frac{\partial p}{\partial z} dz = \int_0^H \varrho \Omega^2 z dz. \tag{5.3}$$

$$-[p(H) - p(0)] = \tfrac{1}{2}\varrho_c \Omega^2 H^2. \tag{5.4}$$

Now, since $p(H) = 0$ and $p(0) = p_c$, we have

$$p_c/\varrho_c = \tfrac{1}{2}\Omega^2 H^2. \tag{5.5}$$

So, in this case there is a factor 1/2 on the right hand side.
Another simple example is the isothermal disc (isothermal in the vertical direction), where $p = c_{\rm s}^2 \varrho_c$. The solution for the vertical structure is

$$\ln \varrho = \ln \varrho_c - \frac{\Omega^2 z^2}{2c_{\rm s}^2} \tag{5.6}$$

In this case the disc extends till infinity, so H has to be defined as the height where ϱ has dropped below a certain value. If we take $\varrho = \varrho_c \exp[-z^2/(2H^2)]$, then we have

$$c_{\rm s}^2 = \frac{p_c}{\varrho_c} = \Omega^2 H^2, \tag{5.7}$$

or

$$c_{\rm s} = \Omega H, \tag{5.8}$$

which is the relation adopted here.

For the present purpose it will suffice to carry out the various vertical integrations by simply replacing

$$\frac{\partial}{\partial z} \rightarrow \pm \frac{1}{H}, \quad z \rightarrow H, \tag{5.9}$$

where H is some disc height and the sign depends on where the differentiated quantity increases or decreases with height. In the case of the pressure, which decreases with height, we have a minus sign, for example. Thus, we have $p_c = \varrho_c g_z H = \varrho_c \Omega^2 H^2$. Here the subscript c refers to central values, ie to the values at the midplane. Since the ratio p/ϱ is the isothermal sound speed, $c_{\rm s}$, we have

$$c_{\rm s} = \Omega H. \tag{5.10}$$

This is a relation that is strictly valid in the case of an isothermal atmosphere (see the box above). The sound speed is related to the central temperature T_c via

$$\frac{\mathcal{R} T_c}{\mu} = c_{\rm s}^2. \tag{5.11}$$

These last two equations, (5.10) and (5.11), are the first two equations governing the structure of accretion discs. Next we need to find an expression that relates the temperature to some other variable. This can be done by considering the radiative equilibrium.

5.2.2 Radiative equilibrium

The disc temperature results from a balance between heating and cooling. The cooling comes from radiative losses. The decrease in thermal energy density is equal to the divergence of the radiative flux, which we introduced in connection with the Sun, see Eq. (3.5).

The *source* of heating in an accretion disc is less obvious. Ultimately, the energy released in the form of radiation comes from the potential energy that is liberated when matter falls towards the central object.

In discs heat is generated by friction. Think for example of a rapidly spinning motor saw. If you press too strongly to the wood it will become hot and start to burn. This is just because of frictional heat and thus proportional to the (dynamical) viscosity μ, which was introduced earlier in connection with friction experienced by a single particle, see Eq. (2.14). The frictional heat must also depend on the velocity gradient between adjacent rings of gas. However, the heat cannot depend on the sign of the shear, so it must be proportional to the square of the shear, so

$$\text{frictional heat} = \text{dynamical viscosity} \times (\text{shear})^2. \tag{5.12}$$

In a rotating system the velocity gradient (ie $\partial u/\partial x$) has to be replaced by the angular velocity gradient multiplied by the cylindrical radius, ie shear $= \varpi \partial\Omega/\partial\varpi$. Those things can be derived rigorously, but here we just try to motivate the various expressions qualitatively.

Thus, the heat generated per unit volume is

$$\text{heat per unit volume} = \mu \left(\varpi \frac{\partial \Omega}{\partial \varpi} \right)^2. \tag{5.13}$$

The dynamical viscosity is the product of gas density ϱ times the so-called kinematic viscosity ν, ie $\mu = \varrho\nu$. As mentioned earlier, in accretion discs one often operates with vertically integrated quantities, so therefore we replace ϱ by σ. Furthermore, since a disc has two surfaces, the heat going into the upper disc plane is only one half of the total, so therefore we have for the

$$\text{heat per unit area} = \tfrac{1}{2} \nu\sigma \left(\tfrac{3}{2} \Omega \right)^2, \tag{5.14}$$

where we have made use of the fact that thin discs rotate according to Kepler's law, $\Omega \sim \varpi^{-3/2}$.

This heat is lost by radiation and the rate of loss is equal to the divergence of the radiative heat flux,

$$F_{\rm rad}(z) = -\frac{16\sigma_{\rm SB}T^3}{3\kappa\varrho}\frac{\partial T}{\partial z}, \tag{5.15}$$

where κ is the opacity. The vertically integrated divergence of $F_{\rm rad}$ is given by $F_{\rm rad}(H)$ minus $F_{\rm rad}(0)$, but $F_{\rm rad}(0)$ vanishes because of symmetry reasons. Before replacing then all variables by vertically integrated quantities we write $4T^3\partial T/\partial z = \partial T^4/\partial z$, so therefore the

$$\text{heat loss per unit area} = F_{\rm rad}(H) = \frac{4\sigma_{\rm SB}T_c^4}{3\kappa\sigma}. \tag{5.16}$$

So the radiative balance equation becomes

$$\frac{4\sigma_{\rm SB}T_c^4}{3\kappa\sigma} = \tfrac{1}{2}\nu\sigma\left(\tfrac{3}{2}\Omega\right)^2. \tag{5.17}$$

Together with equations (5.10) and (5.11) this is the third equation governing the structure of accretion discs. We still need an equation that relates the accretion rate and the viscosity to the remaining variables. In fact, one of the equations not used yet is the equation of angular momentum conservation.

5.2.3 Angular momentum conservation

In general, the rate of change of the angular momentum (AM) density, $\sigma\Omega\varpi^2$, is balanced by the negative divergence of the angular momentum flux, ie

$$\frac{\partial}{\partial t}(\text{rate of change of AM density}) = -\boldsymbol{\nabla}\cdot(\text{AM flux density}) \tag{5.18}$$

The angular momentum flux has no net component in the vertical direction, only in the radial. The radial component of the angular momentum flux consists of two main contributions, one form the advection of angular momentum, ie

$$\text{advected AM} = (2\pi\varpi)\,v_\varpi\,\left(\sigma\varpi^2\Omega\right) = -\dot{M}\varpi^2\Omega. \tag{5.19}$$

The mass flux $\dot{M}$ through a ring at radius ϖ is equal to

$$\dot{M} = -2\pi\int_{-\infty}^{\infty}\varpi\sigma v_\varpi dz = -2\pi\varpi\sigma v_\varpi, \tag{5.20}$$

where the minus sign means that we count the mass flux positive if matter is accreted, ie when the radial velocity v_ϖ is negative.

The other contribution to the radial angular momentum flux is the viscous flux of angular momentum, ie

$$\text{viscous AM flux} = -2\pi\varpi\left(\nu\sigma\varpi^2\frac{\partial\Omega}{\partial\varpi}\right). \tag{5.21}$$

Note that the latter has a minus sign. This is because AM is transported down the gradient of angular velocity.

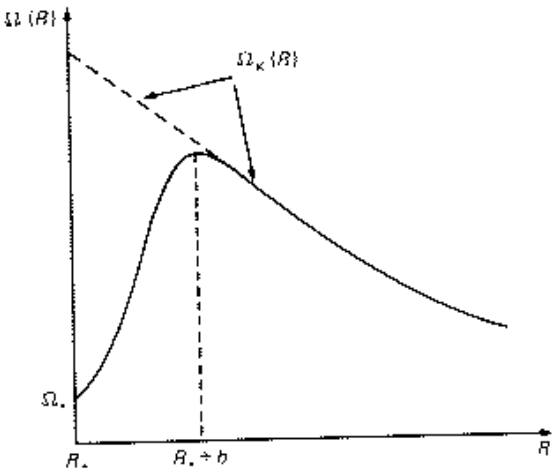

Figure 5.2: Behaviour of $\Omega(\varpi)$ near the surface of the stellar object.

In the steady state the divergence of the sum of the two flux densities vanishes, so the sum of the two fluxes is constant,

$$-\dot{M}\varpi^2\Omega - 2\pi\varpi\left(\nu\sigma\varpi^2\frac{\partial\Omega}{\partial\varpi}\right) = C, \tag{5.22}$$

ie equal to an integration constant C to be determined now.

Near the surface of the central object the angular velocity must match the angular velocity of the star, but because the viscosity is generally small, this will be very near the stellar radius R. So, for $\varpi \approx R$ we have

$$-\dot{M}R^2\Omega(R) = C. \tag{5.23}$$

See illustration in Figure 5.2.

Plugging this into Eq. (5.22) we have

$$-\dot{M}\varpi^2\Omega - 2\pi\varpi\nu\sigma\varpi^2\frac{\partial\Omega}{\partial\varpi} = -\dot{M}R^2\Omega(R). \tag{5.24}$$

Now we use Kepler's law for $\varpi\partial\Omega/\partial\varpi = -\frac{3}{2}\Omega$, so

$$2\pi\nu\sigma\varpi^2(\tfrac{3}{2}\Omega) = \dot{M}\left[\varpi^2\Omega - R^2\Omega(R)\right]. \tag{5.25}$$

Using $\Omega(R)R^2 = \sqrt{GMR}$ we have finally

$$\nu\sigma = \frac{\dot{M}}{3\pi}\left[1 - \left(\frac{R}{\varpi}\right)^{1/2}\right]. \tag{5.26}$$

This is then the fourth equation needed to calculate the radial structure of accretion discs. Let us count the number of unknowns: c_s, H, T_c, σ, κ and ν, so we have altogether 6 unknowns. We need two more equations for the opacity κ and the viscosity ν. Such equations are sometimes called "material equations", because they describe the behaviour of the matter and are exchangeable, unlike three of the other equations with were based on physical conservation laws (vertical and radial momentum together with radiative equilibrium). Equation (5.11) was also a material

equation, because it assumed a perfect gas. [If radiation pressure becomes dominant, for example, this equation will take the form $c_s^2 = (4\sigma_{SB}/c)(T_c^4 H/\sigma)$.]

The expression for κ is complicated, but in principle straightforward, because it is based on atomic physics which is well understood. In general, κ is a function of ϱ and T which has been tabulated. In many cases where only certain absorption processes are important simple formulae can be used. For example, if only free-free transitions are important we can use Kramer's opacity

$$\kappa = \kappa_0 \varrho T^{-7/2}, \tag{5.27}$$

where $\kappa_0 = 6.6 \times 10^{18}\,\mathrm{m^5\,K^{7/2}\,kg^{-2}}$. [This value may well be up to 30 times larger if the gas is "metal rich", ie a good electron supplier, so that bound-free processes become important as well.] This equation is valid at any point, but we shall apply it only to the midplane, so we adopt central values $\kappa = \kappa_0 \varrho_c T_c^{-7/2}$. For very hot gases electron scattering becomes the dominant absorption process. In that case $\kappa = 0.04\,\mathrm{m^2\,kg^{-1}}$ is constant.

Absorption processes in astrophysical plasmas.

- *Electron scattering*: if an electromagnetic wave passes an electron the electric field makes the electron oscillate.
- *Free-free transitions*: if during its thermal motion a free electron passes an ion, the two charged particles form a system which can absorb and emit radiation.
- *Bound-free transitions*: a neutral hydrogen atom in its ground state is ionised by a photon.
- *Bound-bound transitions*: after absorption of a photon the electron jumps to a higher bound state, rather than leaving the atom altogether.
- *Negative Hydrogen ion*: a neutral hydrogen atom is polarised by a nearby charge and can then attract and bind another electron.

[Adapted from Kippenhahn and Weigert (1990).]

The expression for ν is more complicated, because the viscosity is due to some ill-understood turbulent processes. Molecular viscosity would be far too small to cope with the observed accretion rates, cf. Eq. (5.26). By analogy with kinetic gas theory, where the viscosity equals the root-mean-square transport velocity (in general the sound speed) times a mean-free path, we assume that the turbulent viscosity also scales with the sound speed $c_s = \Omega H$ times a fraction α of the disc height H, which is the largest scale an eddy can have, so we write

$$\nu = \alpha \Omega H^2. \tag{5.28}$$

This expression is pretty crude, but it leads to a closed theory of accretion discs which agrees fairly well with observations. This expression was first introduced by Shakura & Sunyaev (1973) and α is therefore sometimes also called α_{SS}. Also, don't confuse this α with the α used in dynamo theory.

Summary of the equations governing the radial structure of accretion discs. There are six equations

$$c_{\rm s} = \Omega H, \tag{5.29}$$

$$\frac{\mathcal{R}T_c}{\mu} = c_{\rm s}^2 \quad \left(= \frac{p_c}{\varrho_c} = \frac{p_c}{\sigma} H\right), \tag{5.30}$$

$$\frac{4\sigma_{\rm SB} T_c^4}{3\kappa\sigma} = \tfrac{1}{2}\nu\sigma \left(\tfrac{3}{2}\Omega\right)^2, \tag{5.31}$$

$$\nu\sigma = \frac{\dot{M}}{3\pi}\left[1 - \left(\frac{R}{\varpi}\right)^{1/2}\right], \tag{5.32}$$

$$\kappa = \kappa_0 \frac{\sigma}{H} T_c^{-7/2}, \tag{5.33}$$

$$\nu = \alpha\Omega H^2, \tag{5.34}$$

for the six unknowns $c_{\rm s}$, H, T_c, σ, κ and ν.

5.2.4 Solution of the disc equations

Solving the system of six algebraic equations in straightforward. First plug in (5.33) into (5.31) to eliminate κ:

$$\frac{4\sigma_{\rm SB} T_c^{15/2} H}{3\kappa_0\sigma^2} = \tfrac{1}{2}\nu\sigma \left(\tfrac{3}{2}\Omega\right)^2. \tag{5.35}$$

Eliminate T_c using (5.30) and move some numerical factors to the right-hand side.

$$\left(\frac{\mathcal{R}}{\mu}\right)^{-15/2} (\Omega H)^{15} H = \frac{27\kappa_0}{32\sigma_{\rm SB}} \nu\sigma^3\Omega^2. \tag{5.36}$$

For abbreviation let us denote

$$\mathcal{K} \equiv \frac{27\kappa_0}{32\sigma_{\rm SB}} \left(\frac{\mathcal{R}}{\mu}\right)^{15/2} \tag{5.37}$$

and eliminate ν using (5.34) we have

$$\Omega^{15} H^{16} = \mathcal{K}\alpha\sigma^3\Omega^3 H^2, \tag{5.38}$$

or

$$H^{14} = \mathcal{K}\alpha\sigma^3\Omega^{-12}. \tag{5.39}$$

This is a relation between H and σ alone, because the other variables are constant ($\mathcal{K}\alpha$) or known functions of radius (Ω). To solve then the whole system of equations we still need another relation between H and σ. This can be obtained by combining (5.32) and (5.34). For abbreviation let us denote

$$\dot{m} \equiv \frac{\dot{M}}{3\pi}\left[1-\left(\frac{R}{\varpi}\right)^{1/2}\right]. \tag{5.40}$$

The term in squared brackets is usually called f^4, so

$$f = \left[1-\left(\frac{R}{\varpi}\right)^{1/2}\right]^{1/4}. \tag{5.41}$$

Eliminating ν from those two equations yields simply

$$\alpha\Omega H^2\sigma = \dot{m}. \tag{5.42}$$

Now eliminating σ from (5.39) and (5.42) yields

$$H^{14} = \mathcal{K}\alpha\left(\dot{m}^3\alpha^{-3}\Omega^{-3}H^{-6}\right)\Omega^{-12}, \tag{5.43}$$

or

$$H^{20} = \mathcal{K}\alpha^{-2}\dot{m}^3\Omega^{-15}, \tag{5.44}$$

or

$$H = \mathcal{K}^{1/20}\alpha^{-1/10}\dot{m}^{3/20}\Omega^{-3/4}. \tag{5.45}$$

Before we proceed with calculating the remaining relations let us now look at some numerical values.

5.2.5 Numerical values

First, using $\sigma_{\rm SB} = 5.67\times10^{-8}\,{\rm W\,m^{-2}\,K^{-4}}$, $\kappa_0 = 6.6\times10^{18}\,{\rm m^5\,K^{7/2}\,kg^{-2}}$, $\mathcal{R} = 8315\,{\rm m^2\,s^{-2}\,K^{-1}}$, and $\mu = 0.62$ we have

$$\mathcal{K} = 8.8\times10^{56}\,{\rm m^{20}\,s^{-12}\,kg^{-3}}. \tag{5.46}$$

Note that $1\,{\rm W} = 1\,{\rm kg\,m^2\,s^{-3}}$, so $\sigma_{\rm SB} = 5.67\times10^{-8}\,{\rm kg\,s^{-3}\,K^{-4}}$. The exact value of α is unknown, because it depends on the nature of the turbulence, for which no theory exists at present. Numerical simulations however indicate that the lower limit is $\alpha = 0.01$, but it is conceivable that α may be much closer to unity. Fortunately, in many expressions α enters only with a relatively small power (see the box below).

Typical values for binaries are $\dot{M} = 10^{13}\,{\rm kg/s}$, so $\dot{m} \approx 10^{12}\,{\rm kg/s}$. We assume $M = 1M_\odot = 2\times10^{30}\,{\rm kg}$ for the central mass. The keplerian angular velocity is then

$$\Omega = \left(\frac{GM}{\varpi^3}\right)^{1/2} \approx \left(\frac{10^{-10}10^{30}}{(10^8)^3}\right)^{1/2}\,{\rm s^{-1}} = 0.01\,{\rm s^{-1}}. \tag{5.47}$$

The exact calculation (with $G = 6.67\times10^{-11}\,{\rm m^3\,kg^{-1}\,s^{-2}}$ and $M = 2\times10^{30}\,{\rm kg}$) yields the value $\Omega = 0.012\,{\rm s^{-1}}$. We can always calculate Ω for other values of the central mass M and distance

from the central mass ϖ, because we know that Ω scales with M to the power $1/2$ and with ϖ to the power $-3/2$, so we may write

$$\Omega = 0.012 \left(\frac{M}{1M_\odot}\right)^{1/2} \left(\frac{\varpi}{10^8\,\mathrm{m}}\right)^{-3/2} \mathrm{s}^{-1}. \tag{5.48}$$

Coming back to Eq. (5.45), let us first calculate the value of the disc height H for the reference values mentioned above. The rough calculation gives

$$H = 10^{58/20} \times 10^{12\times 3/20} \times 0.01^{-3/4}\,\mathrm{m} \approx 10^{2.9+1.8+1.5}\,\mathrm{m} = 10^{6.2}\,\mathrm{m}. \tag{5.49}$$

Again, a more precise calculation yields the value $H = 1.2\times 10^6$ m. To obtain the full dependence on M, $\dot{M}$ and ϖ we simply restore the relevant powers from (5.45) and (5.48), so

$$H = 1.2 \times 10^6 \times \alpha^{-1/10} \left(\frac{\dot{M}f^4}{10^{13}\,\mathrm{kg/s}}\right)^{3/20} \left(\frac{M}{1M_\odot}\right)^{-3/8} \left(\frac{\varpi}{10^8\,\mathrm{m}}\right)^{9/8} \mathrm{m}. \tag{5.50}$$

5.2.6 Temperature

Let us now calculate the scaling of the disc temperature. To do this we make use of relations (5.29) and (5.30)

$$\frac{\mathcal{R}T_c}{\mu} = c_\mathrm{s}^2 = \Omega^2 H^2. \tag{5.51}$$

Since we know Ω and H, we have

$$T = \frac{\mu}{\mathcal{R}} \times 0.012^2 \left(\frac{M}{1M_\odot}\right) \left(\frac{\varpi}{10^8\,\mathrm{m}}\right)^{-3} \times (1.2\times 10^6)^2 \alpha^{-1/5} \left(\frac{\dot{M}f^4}{10^{13}\,\mathrm{kg/s}}\right)^{3/10} \left(\frac{M}{1M_\odot}\right)^{-3/4} \left(\frac{\varpi}{10^8\,\mathrm{m}}\right)^{3/2} \mathrm{K}, \tag{5.52}$$

and with $\mu/\mathcal{R} = (0.62/8315)\,\mathrm{K\,s^2/m^2} \approx 10^{-4}\,\mathrm{K\,s^2/m^2}$ we have

$$T = 1.5 \times 10^4 \times \alpha^{-1/5} \left(\frac{\dot{M}f^4}{10^{13}\,\mathrm{kg/s}}\right)^{3/10} \left(\frac{M}{1M_\odot}\right)^{1/4} \left(\frac{\varpi}{10^8\,\mathrm{m}}\right)^{-3/4} \mathrm{K}. \tag{5.53}$$

This is a temperature similar to that of the Sun. Indeed, in many respects the vertical structure of accretion discs is quite reminiscent of the vertical structure of stars. We can now use this relation to find the temperature at all radii. For example, if the central mass is a neutron star with radius $R = 10\,\mathrm{km} = 10^4$ m, we have a temperature near the surface of the star of $10^4 \times (10^4/10^8)^{-3/2}\,\mathrm{K} = 10^7\,\mathrm{K}$.

5.2.7 The surface density

To calculate σ we can use equations (5.32) and (5.34), so

$$\sigma = \dot{m}\nu^{-1} = \dot{m}\alpha^{-1}\Omega^{-1}H^{-2}. \tag{5.54}$$

Using (5.48) and (5.50) we have

$$\sigma = 1.1 \times 10^{12} \times \left(\frac{\dot{M}f^4}{10^{13}\,\mathrm{kg/s}}\right) \alpha^{-1}(0.012)^{-1} \left(\frac{M}{1M_\odot}\right)^{-1/2} \left(\frac{\varpi}{10^8\,\mathrm{m}}\right)^{3/2}$$
$$\times (1.2 \times 10^6)^{-2} \times \alpha^{1/5} \left(\frac{\dot{M}f^4}{10^{13}\,\mathrm{kg/s}}\right)^{-3/10} \left(\frac{M}{1M_\odot}\right)^{3/4} \left(\frac{\varpi}{10^8\,\mathrm{m}}\right)^{-9/4} \mathrm{kg\,m^{-2}}. \quad (5.55)$$

This gives

$$\sigma = 61 \times \alpha^{-4/5} \left(\frac{\dot{M}f^4}{10^{13}\,\mathrm{kg/s}}\right)^{7/10} \left(\frac{M}{1M_\odot}\right)^{1/4} \left(\frac{\varpi}{10^8\,\mathrm{m}}\right)^{-3/4} \mathrm{kg\,m^{-2}}. \quad (5.56)$$

5.2.8 The pressure

Using (5.29) and (5.30) we see that the pressure is given by

$$p_c = \Omega^2 H \sigma \quad (5.57)$$

ie

$$p_c = (0.012)^2 \left(\frac{M}{1M_\odot}\right) \left(\frac{\varpi}{10^8\,\mathrm{m}}\right)^{-3} 1.2 \times 10^6 \times \alpha^{-1/10} \left(\frac{\dot{M}f^4}{10^{13}\,\mathrm{kg/s}}\right)^{3/20} \left(\frac{M}{1M_\odot}\right)^{-3/8} \left(\frac{\varpi}{10^8\,\mathrm{m}}\right)^{9/8}$$
$$\times 61 \times \alpha^{-4/5} \left(\frac{\dot{M}f^4}{10^{13}\,\mathrm{kg/s}}\right)^{7/10} \left(\frac{M}{1M_\odot}\right)^{1/4} \left(\frac{\varpi}{10^8\,\mathrm{m}}\right)^{-3/4} \mathrm{kg\,m^{-1}\,s^{-2}} \quad (5.58)$$

$$p_c = 1.1 \times 10^4 \times \alpha^{-9/10} \left(\frac{\dot{M}f^4}{10^{13}\,\mathrm{kg/s}}\right)^{-3/20} \left(\frac{M}{1M_\odot}\right)^{7/8} \left(\frac{\varpi}{10^8\,\mathrm{m}}\right)^{-21/8} \mathrm{kg\,m^{-1}\,s^{-2}} \quad (5.59)$$

Full solution:

$$H = 1.2 \times 10^6 \times \alpha^{-1/10} \left(\frac{\dot{M}f^4}{10^{13}\,\mathrm{kg/s}}\right)^{3/20} \left(\frac{M}{1M_\odot}\right)^{-3/8} \left(\frac{\varpi}{10^8\,\mathrm{m}}\right)^{9/8} \mathrm{m}. \quad (5.60)$$

$$T = 1.5 \times 10^4 \times \alpha^{-1/5} \left(\frac{\dot{M}f^4}{10^{13}\,\mathrm{kg/s}}\right)^{3/10} \left(\frac{M}{1M_\odot}\right)^{1/4} \left(\frac{\varpi}{10^8\,\mathrm{m}}\right)^{-3/4} \mathrm{K}. \quad (5.61)$$

$$\sigma = 61 \times \alpha^{-4/5} \left(\frac{\dot{M}f^4}{10^{13}\,\mathrm{kg/s}}\right)^{7/10} \left(\frac{M}{1M_\odot}\right)^{1/4} \left(\frac{\varpi}{10^8\,\mathrm{m}}\right)^{-3/4} \mathrm{kg\,m^{-2}}. \quad (5.62)$$

$$p_c = 1.1 \times 10^4 \times \alpha^{-9/10} \left(\frac{\dot{M}f^4}{10^{13}\,\mathrm{kg/s}}\right)^{17/20} \left(\frac{M}{1M_\odot}\right)^{7/8} \left(\frac{\varpi}{10^8\,\mathrm{m}}\right)^{-21/8} \mathrm{kg\,m^{-1}\,s^{-2}} \quad (5.63)$$

In the derivation we have omitted the contribution of the radiation pressure to the total pressure. In general we would have to replace the pressure by the sum of the gas pressure $p_{\rm gas} = (\mathcal{R}/\mu)T\varrho$ and radiation pressure, $p_{\rm rad} = \frac{4\sigma_{\rm SB}}{3c}T^4$. If $p_{\rm rad} \ll p_{\rm gas}$ we can neglect the radiation pressure. To see whether this is the case we compute $p_{\rm rad}$ for the standard disc solution:

$$p_{\rm rad} = \frac{4\sigma_{\rm SB}}{3c}T^4 = 13 \times \alpha^{-4/5} \left(\frac{\dot{M}f^4}{10^{13}\,{\rm kg/s}}\right)^{6/5} \left(\frac{M}{1M_\odot}\right) \left(\frac{\varpi}{10^8\,{\rm m}}\right)^{-3} {\rm kg\,m^{-1}\,s^{-2}}. \tag{5.64}$$

This value is much smaller than $p_{\rm gas}$ at the same radius. To see how this changes as we go further in let us calculate the ratio

$$\frac{p_{\rm rad}}{p_{\rm gas}} = 1.2 \times 10^{-3} \times \alpha^{1/10} \left(\frac{\dot{M}f^4}{10^{13}\,{\rm kg/s}}\right)^{7/20} \left(\frac{M}{1M_\odot}\right)^{1/8} \left(\frac{\varpi}{10^8\,{\rm m}}\right)^{-3/8}. \tag{5.65}$$

Obviously, this ratio is small. Only for $\varpi \approx 1.6\,{\rm m}$ (ie way into the central object itself!) does it become comparable to unity.

5.2.9 The opacity

Similar to the pressure, the opacity too has (at least) two different contributions: Kramer's opacity, $\kappa_{\rm Kr}$, and the opacity for electron scattering, $\kappa_{\rm es}$. The latter is constant ($= 0.04\,{\rm m^2\,kg^{-1}}$), ie independent of ϱ and T. In order to see when electron scattering becomes important, let us calculate $\kappa_{\rm Kr}$ for the standard solution:

$$\kappa_{\rm Kr} = \kappa_0 \sigma H^{-1} T^{-7/2}, \tag{5.66}$$

$$\kappa_{\rm Kr} = 0.82 \times \left(\frac{\dot{M}f^4}{10^{13}\,{\rm kg/s}}\right)^{-1/2} \left(\frac{M}{1M_\odot}\right)^{-1/4} \left(\frac{\varpi}{10^8\,{\rm m}}\right)^{3/4} {\rm m^2\,kg^{-1}}. \tag{5.67}$$

Note that this expression is *independent* of α. We see that only for $\varpi \leq 1.8 \times 10^6\,{\rm m}$ does electron scattering become important.

Chapter 6

Active Galaxies and Quasars

In this chapter much more should be said, but we there was not enough time to cover it all. Several points will just be mentioned very briefly. Most of the space is devoted to the nuclei of so-called active galaxies. They are the engine of quasars — quasi-stellar (point-like) objects, and are among the brightest objects in the sky. Quasars have been somewhat of a mystery since they were discovered in 1963, but now we know that they are basically just accretion discs on a gigantic scale around a supermassive back hole. They are very far away, at cosmological distances, and have redshifts of $z = 0.1$ till $z = 5$. (Because the Universe is expanding, the further something is away, the faster it runs away from us, so the larger is the redshift. For $z = 0.16$, as in the quasar 3C273, the redshift is 16%, whilst for $z = 5$ the entire electromagnetic spectrum is rescaled by a factor of 5.) It is really because of those large distances that quasars look pointlike. However, now with the Hubble Space Telescope (HST) it has been possible to say that all quasars are really within more-or-less ordinary looking galaxies. Therefore we now believe that when the Universe was a few 10^8 yr old, most galaxies must have gone through a phase where they had a quasar in their centre.

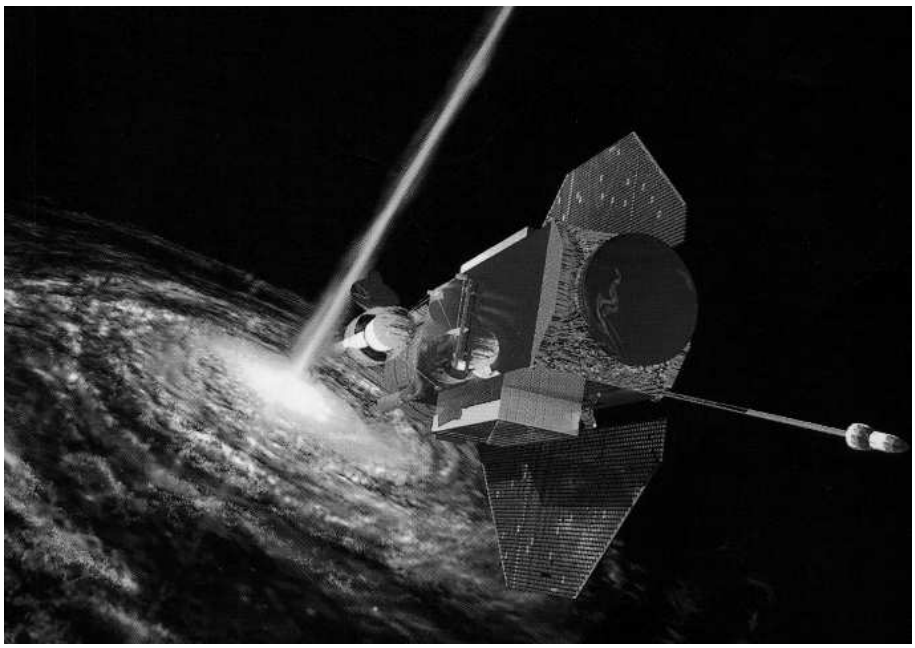

Figure 6.1: Artist's impression of an accretion disc with a jet.

Figure 6.1 gives an artist's impression of an accretion disc around a supermassive black hole. A real active galactic nuclei is shown in Figure 6.2.

6.1 Pretty pictures from the web

The Hubble Space Telescope has now been able to provide direct images of accretion discs. An especially fascinating picture is that of M87; Figure 6.2. A full list of items is available under the URL

`http://opposite.stsci.edu/pubinfo/pictures.html`

6.2 Active galactic nuclei

The luminosity of an AGN is about 100 times larger than the luminosity of ordinary galaxies. There are actually objects that are even brighter than AGNs, but only for a very short time. Those objects are gamma-ray bursters, whose nature we are only now beginning to understand, even though they have been detected over 20 years ago when people were looking for gamma ray bursts originating from H-bomb ignitions.

Typical masses of AGNs are around 10^8 solar masses. It has long be a mystery how a luminosity of 10^{13} solar luminosities could be explained. The mass-luminosity relation for galaxies is approximately linear, ie $L \sim M^n$ with $n \approx 1$, so this would not suffice to explain the enormous luminosities of quasars. Stars have a nonlinear mass-luminosity relation, $L \sim M^3$ for main sequence stars, which could yield sufficient luminosity for objects of 10^8 solar masses, if that relation was actually valid for quasars. However, there are serious stability problems when trying to explain so massive objects in terms of superluminous stars. In fact, for stars exceeding 50 solar masses the radiation pressure becomes so immense that it would blow away the star's atmosphere if the luminosity exceeded the $L \sim M$ relation.

The reason why accretion discs can explain such high luminosities is because they can release huge amounts of binding energy. A body of mass m that falls onto another object of mass M gains kinetic energy that is equal to the potential energy, which is

$$E = \frac{GM}{R}\, m. \tag{6.1}$$

If mass falls in at a rate $\dot{M}$ the rate of energy release is

$$L \equiv \dot{E} = \frac{GM}{R}\dot{M}. \tag{6.2}$$

The smaller the central body, and the more massive it is, the larger will be the energy release. The smallest and yet massive bodies are black holes. The Schwarzschild radius is $2GM/c^2$, where c is the speed of light, and if we identify this with R we have

$$L \equiv \dot{E} = \tfrac{1}{2}c^2\dot{M}. \tag{6.3}$$

For accretion rates of 2 solar masses per year this amounts to

$$L \equiv \dot{E} = 0.5\,(3\times 10^8)^2\,\frac{2\times 2\times 10^{30}}{3\times 10^7} \approx 10^{17}\,10^{23} = 10^{40}\,\mathrm{W}, \tag{6.4}$$

which would fit the observed luminosities of quasars very well. (10^{13} solar luminosities correspond to approximately $10^{13}\times 4\times 10^{26}\,\mathrm{W} = 4\times 10^{39}\,\mathrm{W}$.) The remarkable thing here is that such a

mechanism can lead to energies very close to the rest mass energy, Mc^2. Note that nuclear fusion is much less efficient: here the energy generated is only $0.007 \times Mc^2$. In that sense one can say that black hole accretion discs are more powerful than nuclear fusion! In the following we consider the properties of such discs in more detail.

6.3 AGN discs

In this section we use the standard accretion disc equations, but rescaled to the parameters applicable to active galactic nuclei:

$$\dot{M} = 10^{23}\,\mathrm{kg\,s^{-1}}, \quad M = 10^8 M_\odot = 2 \times 10^{38}\,\mathrm{kg}, \quad \varpi = 10^{12}\,\mathrm{m} \qquad \text{(for AGNs)}. \tag{6.5}$$

An important length scale here is the Schwarzschild radius, $R_S = GM/(2c^2)$, where $c = 3 \times 10^8\,\mathrm{m/s}$ is the speed of light. It would not be meaningful to consider disc radii smaller than R_S. For 10^8 solar masses this radius is $R_S = 7.4 \times 10^{10}\,\mathrm{m}$.

Let us first calculate the orbital frequency for those values:

$$\Omega = \sqrt{\frac{GM}{\varpi^3}} = \sqrt{\frac{6.67 \times 10^{-11} \times 2 \times 10^{38}}{(10^{12})^3}} = 1.2 \times 10^{-4} \left(\frac{M}{10^8 M_\odot}\right)^{1/2} \left(\frac{\varpi}{10^{12}\,\mathrm{m}}\right)^{-3/2} \mathrm{s^{-1}}. \tag{6.6}$$

In order to obtain the disc height H for the parameters (6.5) we just plug in those numbers into Eq. (5.50)

$$H_{\mathrm{AGN}} = 1.2 \times 10^6 \times \left(\frac{10^{23}\,\mathrm{kg/s}}{10^{13}\,\mathrm{kg/s}}\right)^{3/20} \left(\frac{10^8 M_\odot}{1 M_\odot}\right)^{-3/8} \left(\frac{10^{12}\,\mathrm{m}}{10^8\,\mathrm{m}}\right)^{9/8} \mathrm{m} = 1.2 \times 10^9\,\mathrm{m}. \tag{6.7}$$

Restoring now the full dependence on the various parameters we have

$$H = 1.2 \times 10^9 \times \alpha^{-1/10} \left(\frac{\dot{M} f^4}{10^{23}\,\mathrm{kg/s}}\right)^{3/20} \left(\frac{M}{10^8 M_\odot}\right)^{-3/8} \left(\frac{\varpi}{10^{12}\,\mathrm{m}}\right)^{9/8} \mathrm{m}. \tag{6.8}$$

For the temperature we calculate first the value for the AGN parameters using Eq. (5.61)

$$T_{\mathrm{AGN}} = 1.5 \times 10^4 \times \left(\frac{10^{23}\,\mathrm{kg/s}}{10^{13}\,\mathrm{kg/s}}\right)^{3/10} \left(\frac{10^8 M_\odot}{1 M_\odot}\right)^{1/4} \left(\frac{10^{12}\,\mathrm{m}}{10^8\,\mathrm{m}}\right)^{-3/4} \mathrm{K} = 10^6\,\mathrm{K}. \tag{6.9}$$

Again, restoring the full dependence on parameters we have

$$T = 1.5 \times 10^6 \times \alpha^{-1/5} \left(\frac{\dot{M} f^4}{10^{23}\,\mathrm{kg/s}}\right)^{3/10} \left(\frac{M}{10^8 M_\odot}\right)^{1/4} \left(\frac{\varpi}{10^{12}\,\mathrm{m}}\right)^{-3/4} \mathrm{K}. \tag{6.10}$$

Now for the surface density, we have from Eq. (5.62)

$$\sigma_{\mathrm{AGN}} = 61 \times \left(\frac{10^{23}\,\mathrm{kg/s}}{10^{13}\,\mathrm{kg/s}}\right)^{7/10} \left(\frac{10^8 M_\odot}{1 M_\odot}\right)^{1/4} \left(\frac{10^{12}\,\mathrm{m}}{10^8\,\mathrm{m}}\right)^{-3/4} \mathrm{kg\,m^{-2}} = 6.1 \times 10^7\,\mathrm{kg\,m^{-2}}. \tag{6.11}$$

and so the general formula is

$$\sigma = 6.1 \times 10^7 \times \alpha^{-4/5} \left(\frac{\dot{M} f^4}{10^{23}\,\mathrm{kg/s}}\right)^{7/10} \left(\frac{M}{10^8 M_\odot}\right)^{1/4} \left(\frac{\varpi}{10^{12}\,\mathrm{m}}\right)^{-3/4} \mathrm{kg\,m^{-2}}. \tag{6.12}$$

Finally for the pressure we have from Eq. (5.63)

$$p_c^{\rm AGN} = 1.1\times 10^4 \times \left(\frac{10^{23}\,{\rm kg/s}}{10^{13}\,{\rm kg/s}}\right)^{-3/20} \left(\frac{10^8 M_\odot}{1 M_\odot}\right)^{7/8} \left(\frac{10^{12}\,{\rm m}}{10^8\,{\rm m}}\right)^{-21/8} {\rm kg\,m^{-1}\,s^{-2}} 1.1\times 10^9\,{\rm kg\,m^{-1}\,s^{-2}} \tag{6.13}$$

$$p_c = 1.1\times 10^9 \times \alpha^{-9/10} \left(\frac{\dot M f^4}{10^{23}\,{\rm kg/s}}\right)^{-3/20} \left(\frac{M}{10^8 M_\odot}\right)^{7/8} \left(\frac{\varpi}{10^{12}\,{\rm m}}\right)^{-21/8} {\rm kg\,m^{-1}\,s^{-2}} \tag{6.14}$$

In this case the ratio of radiation pressure and gas pressure is

$$\frac{p_{\rm rad}}{p_{\rm gas}} = 1.2\times \alpha^{1/10} \left(\frac{\dot M f^4}{10^{23}\,{\rm kg/s}}\right)^{7/20} \left(\frac{M}{10^8 M_\odot}\right)^{1/8} \left(\frac{\varpi}{10^{12}\,{\rm m}}\right)^{-3/8} \tag{6.15}$$

Note that this ratio is no longer small. Clearly, effects of the radiative pressure begin to be important and should be taken into account for more accurate considerations.

Electron scattering becomes important when the Kramer opacity drops below the value $0.04\,{\rm m^2\,kg^{-1}}$. Rescaling Eq. (5.67) for values relevant for AGNs we have

$$\kappa_{\rm Kr} = 8.2\times 10^{-5} \times \left(\frac{\dot M f^4}{10^{23}\,{\rm kg/s}}\right)^{-1/2} \left(\frac{M}{10^8 M_\odot}\right)^{-1/4} \left(\frac{\varpi}{10^{12}\,{\rm m}}\right)^{3/4} {\rm m^2\,kg^{-1}}. \tag{6.16}$$

Thus, electron scattering is always important. Only for $\varpi \geq 4\times 10^{15}\,{\rm m}$ does Kramer's opacity dominate over electron scattering. Since electron scattering is important in most parts of the disc we give for this case the solution in the box below.

Accretion disc solution for the case when electron scattering dominates over Kramer's opacity:

$$H = 2.4\times 10^9 \times \alpha^{-1/10} \left(\frac{\dot M f^4}{10^{23}\,{\rm kg/s}}\right)^{1/5} \left(\frac{M}{10^8 M_\odot}\right)^{-7/20} \left(\frac{\varpi}{10^8\,{\rm m}}\right)^{21/20} {\rm m}. \tag{6.17}$$

$$T = 6.2\times 10^6 \times \alpha^{-1/5} \left(\frac{\dot M f^4}{10^{23}\,{\rm kg/s}}\right)^{2/5} \left(\frac{M}{10^8 M_\odot}\right)^{3/10} \left(\frac{\varpi}{10^8\,{\rm m}}\right)^{-9/10} {\rm K}. \tag{6.18}$$

$$\sigma = 1.5\times 10^7 \times \alpha^{-4/5} \left(\frac{\dot M f^4}{10^{23}\,{\rm kg/s}}\right)^{3/5} \left(\frac{M}{10^8 M_\odot}\right)^{1/5} \left(\frac{\varpi}{10^8\,{\rm m}}\right)^{-3/5} {\rm kg\,m^{-2}}. \tag{6.19}$$

$$\kappa_{\rm Kr} = 7\times 10^{-8} \times \left(\frac{\dot M f^4}{10^{23}\,{\rm kg/s}}\right)^{-1} \left(\frac{M}{10^8 M_\odot}\right)^{-1/2} \left(\frac{\varpi}{10^{12}\,{\rm m}}\right)^{3/2} {\rm m^2\,kg^{-1}}. \tag{6.20}$$

With this expression, only for $\varpi \geq 7\times 10^{15}\,{\rm m}$ does Kramer's opacity dominate over electron scattering.

We see that AGN discs are so hot that they must radiate mostly in X-rays.

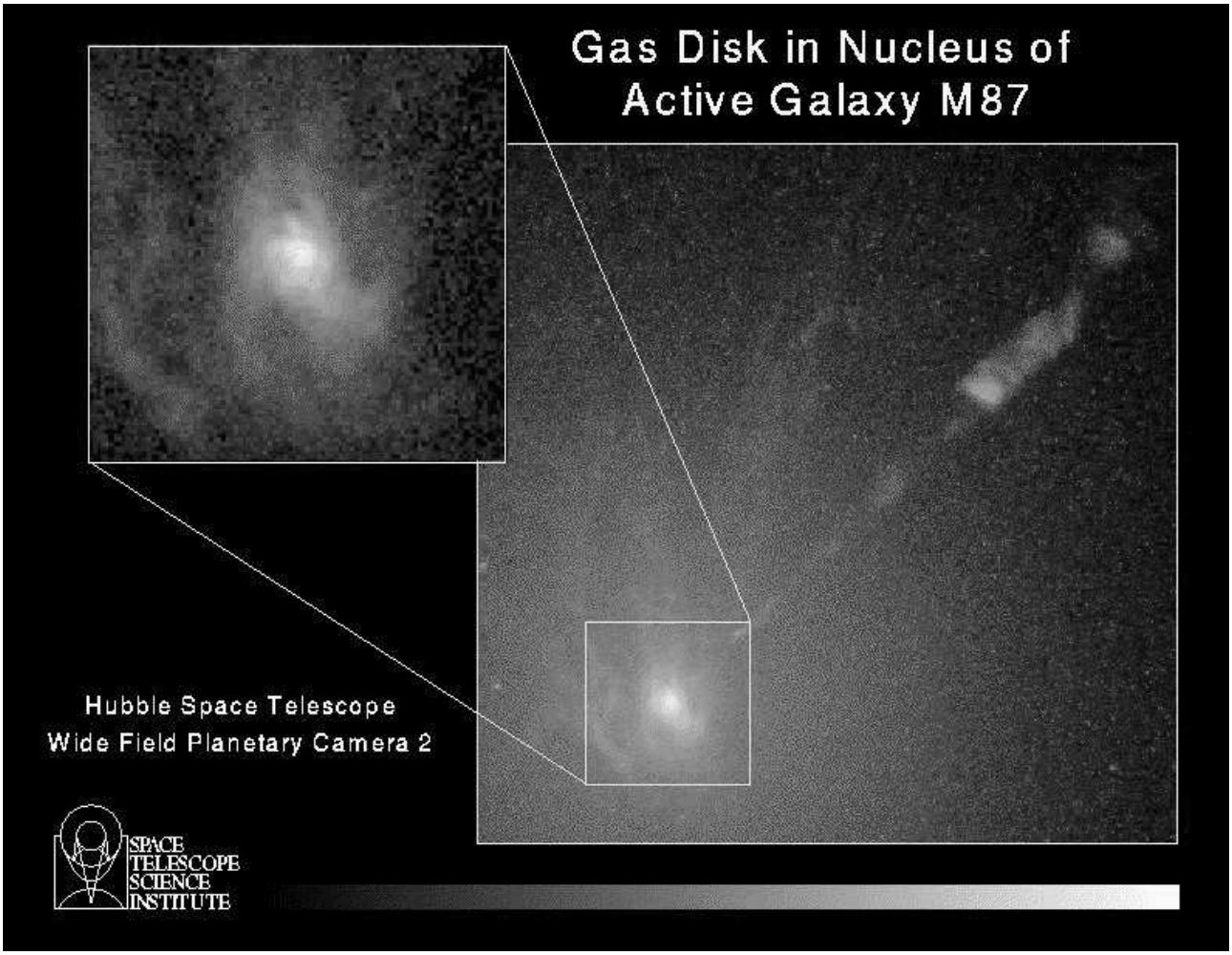

Figure 6.2: The gas disc of the nucleus of the active galaxy M87 together with its jet. The full press release that goes with this picture is reproduced in § 6.4.

6.4 M87, an example of

6.4.1 M87: a nearby active galaxy

Chapter 7

Jets

It seems that all accretion discs have a jet. Apparently, all discs also have a magnetic field. There is a mechanism for launching jets that relies on the centrifugal force in the disc. If the field sticks out of the disc at a suitable angle then the disc material can be tossed away along the field line. The field lines really act like tubes along which material can flow freely, but not perpendicular to it. This picture applies only if the conductivity is large (which is practically always the case) and if the kinetic energy density is weak compared with the magnetic energy density. In the following section we discuss the angle the field lines must have for the launching mechanism to work.

7.1 Centrifugal launching

Suppose the field line is anchored at a radius R. At some position (x, z) with $\varpi = R + x$ the centrifugal force is given by

$$\mathbf{F}_{\rm centrif} = \Omega_0^2 \begin{pmatrix} R+x \\ 0 \\ 0 \end{pmatrix} . = \Omega_0^2 R \begin{pmatrix} 1+\tilde{x} \\ 0 \\ 0 \end{pmatrix}, \tag{7.1}$$

where $\tilde{x} = x/R$. The gravitational force is given by

$$\mathbf{F}_{\rm grav} = -\frac{GM}{r^3} \begin{pmatrix} R+x \\ 0 \\ z \end{pmatrix}, \tag{7.2}$$

but since $r \approx R + x$ to first order[1] we have

$$\mathbf{F}_{\rm grav} \approx -\frac{GM}{R^2} \begin{pmatrix} 1-2\tilde{x} \\ 0 \\ \tilde{z} \end{pmatrix}, \tag{7.3}$$

so their sum gives (remembering that $\Omega_0^2 = GM/R^3$)

$$\mathbf{F} \equiv \mathbf{F}_{\rm centrif} + \mathbf{F}_{\rm grav} = \Omega_0^2 R \begin{pmatrix} 3\tilde{x} \\ 0 \\ -\tilde{z} \end{pmatrix}. \tag{7.4}$$

[1] We consider the vicinity of a thin disc here

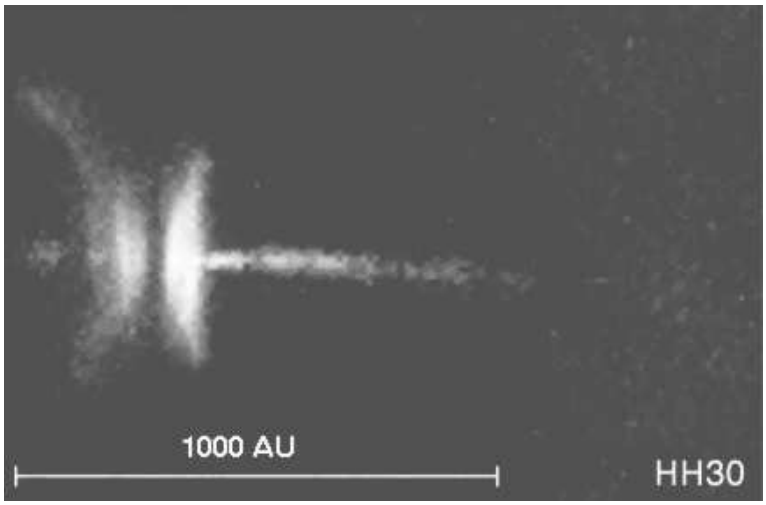

Figure 7.1: The object HH30 showing a protostellar accretion disc with a jet emanating along the disc axis.

To calculate the force along the field line, we have to project the component of $\mathbf{F}$ onto the field vector. Assume that the field line is tilted against the vertical direction by an angle i, then the unit vector, $\hat{\mathbf{B}}$, along the B-field is

$$\hat{\mathbf{B}} = \begin{pmatrix} \sin i \\ 0 \\ \cos i \end{pmatrix} \tag{7.5}$$

and so the force along the field line is

$$F_B = \hat{\mathbf{B}} \cdot \mathbf{F} = \Omega_0^2 R_0 (3\tilde{x} \sin i - \tilde{z} \cos i) \tag{7.6}$$

or, since $\tilde{x} = \tilde{z} \tan i$,

$$F_B = \Omega_0^2 R_0 \tilde{z} \cos i \, [3(\tan i)^2 - 1]. \tag{7.7}$$

Thus, for $i = \text{atan}(1/\sqrt{3}) = 30^\circ$ we have $F_B = 0$. For opening angles larger than 30° we have $F_B > 0$, ie matter will flow away from the disc. In practice the opening angles cannot be too large, because then the disc will lose its matter too quickly. Recent simulations[2] show that the field lines have a tendency to adjust themselves to the critical angle. This shows that the jet is really centrifugally launched, and that the field line angle is somehow self regulated.

7.2 Magnetic collimation

7.3 Superluminal motion

Jets from AGNs move extremely fast, with gas velocities very close to the speed of light c. Sometimes they even seem to be ten times faster than light, cf Figure 7.2. The quasar 3C 273 depicted there emits a bright "knot" that has moved over a distance of about 10 light years in one year's time.

[2]See the paper in *Nature*, **385**, p. 409 by R. Ouyed, R. E. Pudritz and J. M. Stone (1997)

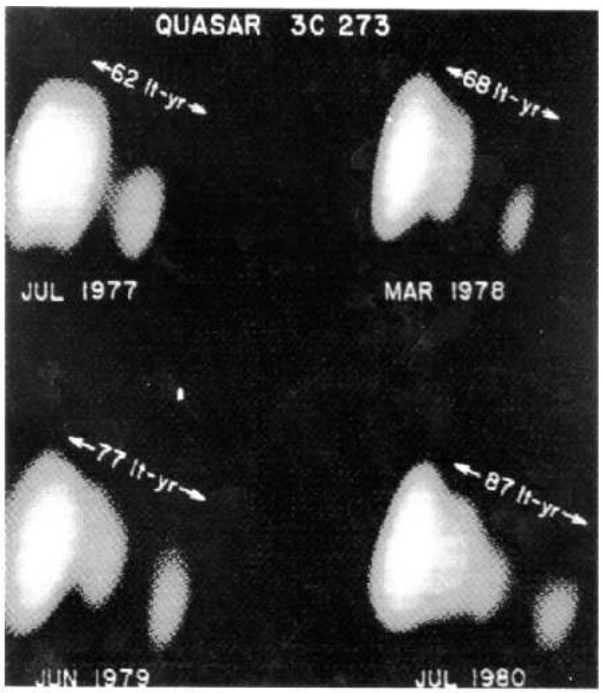

Figure 7.2: Superluminal motion of structures ("knots") in the jet ejected from the quasar 3C 273. Shown are infrared images obtained at different times. The jet itself is not visible, but the knot moves along it.

This puzzled researchers for quite some time, but finally they found the following explanation, illustrated in Figure 7.3: The jet moves almost towards the observer (that is, us), the inclination of the jet axis relative to the line of sight being only $\approx 8°$. When the knot is emitted from the central object, the light showing it at the centre starts traveling at a speed $v = c$ towards the observer — of course, light propagates in all directions, but only this ray we will eventually see; let us call it the 'initial picture'. At the same time, the knot travels with a speed $v \approx c$ (but still $v < c$; typical values are 95–99% of c) along the jet axis.

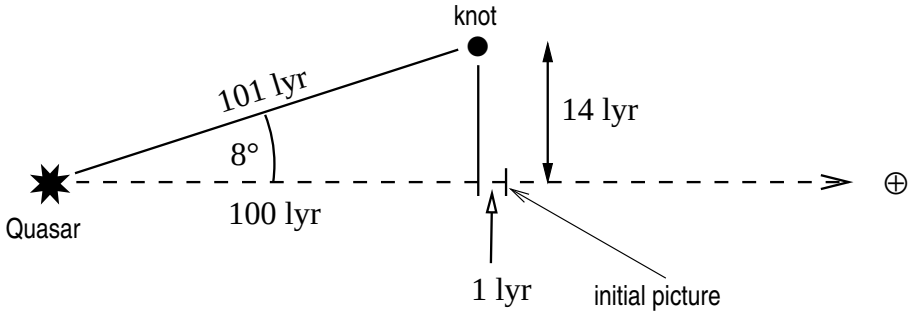

Figure 7.3: Geometry of the Quasar 3C 273 and the observer (⊕).

This means that *the knot almost keeps its initial distance from the 'initial picture'*, and after 101 years, when the initial picture approached the observer by 101 lyr [light years], the knot has made 100 lyr in the direction of the observer. Hence, the initial picture is just one light year ahead of the second picture that shows the knot in the new position. Accordingly we observe the second picture one year later than the initial one — although in reality is has been emitted 101 years later. Since we can observe only motions in the plane perpendicular to the line of

sight, we interpret their angular separation as a distance of 14 lyr, apparently gained in just one year's time.

It is easy to apply this explanation to a more general geometry: Assume that jet moves with $v \approx c$ at a small angle α (NB: $8^\circ = 0.14\,\mathrm{rad}$ *is* small) relative to the line of sight. After a time l/c, both the knot and the initial picture have travelled a distance of l (in Figure 7.3, $l = 101$ lyr). Thereby, the knot has travelled $l_{||} = l\cos\alpha$ along the line of sight ($l_{||} = 100$ lyr in the example) and $l_\perp = l\sin\alpha \approx l\alpha$ ($l_\perp = 14$ lyr in the example) perpendicular to it. Hence, the initial picture is $\Delta l = l - l\cos\alpha \approx l\alpha^2/2$ ahead of the second picture and we will see a time lag $\Delta t \approx \Delta l/c$ between the two pictures. The apparent velocity is then given by

$$v_{\mathrm{app}} = \frac{l_\perp}{\Delta l}c \approx \frac{l\alpha}{l\alpha^2/2}c \approx \frac{2c}{\alpha}. \tag{7.8}$$

For $\alpha = 8^\circ$ we recover the value $v_{\mathrm{app}} \approx 14c$, but obviously for smaller α we can even have much higher apparent velocities, if the objects can still be separated by the telescope.

There is some analogy between this apparent superluminal motion and the classical example of the light beam from a lighthouse that can move at superluminal velocity, too. Consider a lighthouse where the lamp rotates once each 30 s, corresponding to an angular frequency $\omega \approx 0.2\ \mathrm{s}^{-1}$. The bright spot marked by the light on a wall at a distance r will move at a velocity $v = \omega r$. Hence, at a distance r greater than $c/\omega \approx 1.6$ million kilometers, the bright spot will move faster than light. The distance above is about four times the distance between the lighthouse and the Moon, but with a laser pointer you can easily increase ω by more than a factor of four and can thus make a bright "little" red spot move superluminally over the Moon's surface.

If you really try this, you will find that no hand appears in the sky to keep you from violating nature's laws. In fact you don't violate them: Special relativity tells us that matter (energy) and information cannot move faster than light. But your little red spot does not carry matter, nor does it represent a signal moving over the Moon's surface. It *is* caused by a signal, but rather one that propagates from the pointer in your hand up to the Moon, and moves at, but not faster than, the speed of light.

Similarly, in Figure 7.3 the initial picture cannot influence the emission of the second picture by the knot. Their causal link originates 101 yr back in time and consists in a common cause, rather than a unidirectional causal influence.

Chapter 8

Appendix

8.1 Disc solution with radiation pressure

The expression for the pressure should, in addition to the gas pressure $p_{\rm gas} = (\mathcal{R}/\mu)T\varrho$, also include the additional term for the radiation pressure, $p_{\rm rad} = \frac{4\sigma_{\rm SB}}{3c}T^4$. Here we shall only consider the limiting case $p_{\rm rad} \gg p_{\rm gas}$. Thus, Eq. (5.30) has to be replaced by

$$c_{\rm s}^2 = \frac{p}{\varrho} = \frac{4\sigma_{\rm SB}}{3c}\frac{T^4}{\varrho}, \tag{8.1}$$

and because of Eq. (5.29) we have

$$\Omega^2 H^2 = c_{\rm s}^2 = \frac{4\sigma_{\rm SB}}{3c}\frac{T_c^4}{\varrho_c}. \tag{8.2}$$

Using $\varrho_c = \sigma/H$ we have

$$\Omega^2 H = \frac{4\sigma_{\rm SB}}{3c}\frac{T_c^4}{\sigma}. \tag{8.3}$$

So

$$T_c = \left(\frac{3c}{4\sigma_{\rm SB}}\Omega^2 H\sigma\right)^{1/4} \tag{8.4}$$

On the other hand, from Equations (5.31) and (5.33) we have

$$T_c^{15/2} = \frac{27\kappa_0}{32\sigma_{\rm SB}}\nu\sigma^3\Omega^2 H^{-1}, \tag{8.5}$$

or

$$T_c = \left(\frac{27\kappa_0}{32\sigma_{\rm SB}}\alpha\sigma^3\Omega^3 H\right)^{2/15}, \tag{8.6}$$

Combining this with (8.4) to eliminate T_c yields

$$\left(\frac{3c}{4\sigma_{\rm SB}}\Omega^2 H\sigma\right)^{1/4} = T_c = \left(\frac{27\kappa_0}{32\sigma_{\rm SB}}\alpha\sigma^3\Omega^3 H\right)^{2/15}, \tag{8.7}$$

or

$$\left(\frac{3c}{4\sigma_{\rm SB}}\Omega^2 H\sigma\right)^{15} = \left(\frac{27\kappa_0}{32\sigma_{\rm SB}}\alpha\sigma^3\Omega^3 H\right)^8. \tag{8.8}$$

Thus

$$\left(\frac{3c}{4\sigma_{\rm SB}}\right)^{15}\Omega^{30}H^{15}\sigma^{15} = \left(\frac{27\kappa_0}{32\sigma_{\rm SB}}\right)^8\alpha^8\sigma^{24}\Omega^{24}H^8, \tag{8.9}$$

$$H^7 = \frac{(27\kappa_0)^8\sigma_{\rm SB}^7}{4^{21}}\alpha^8\Omega^{-6}\sigma^9, \tag{8.10}$$

Use $\alpha\Omega H^2\sigma = \dot{m}$ to eliminate σ we have

$$H^7 = \tilde{\mathcal{K}}\alpha^8\Omega^{-6}\dot{m}^9\alpha^{-9}\Omega^{-9}H^{-18} \tag{8.11}$$

where

$$\tilde{\mathcal{K}} = \left(\frac{27\kappa_0}{32\sigma_{\rm SB}}\right)^8\left(\frac{4\sigma_{\rm SB}}{3c}\right)^{15}\,{\rm m}^{25}\,{\rm kg}^{-9}\,{\rm s}^{-6}\,{\rm K}^{-28} = \frac{(27\kappa_0)^8}{(3c)^{15}}\frac{\sigma_{\rm SB}^7}{4^5}\,{\rm m}^{25}\,{\rm kg}^{-9}\,{\rm s}^{-6}\,{\rm K}^{-28} \tag{8.12}$$

is a constant. Thus

$$H^{25} = \tilde{\mathcal{K}}\alpha^{-1}\dot{m}^9\Omega^{-15} \tag{8.13}$$

or

$$H = \tilde{\mathcal{K}}^{1/25}\alpha^{-1/25}\dot{m}^{9/25}\Omega^{-3/5} \tag{8.14}$$

Using again $\alpha\Omega H^2\sigma = \dot{m}$ to calculate σ we obtain

$$\sigma = \dot{m}\alpha^{-1}\Omega^{-1}H^{-2}, \tag{8.15}$$

ie

$$\sigma = 1.1\times10^5\times\alpha^{-23/25}\left(\frac{\dot{M}f^4}{10^{13}\,{\rm kg/\,s}}\right)^{7/25}\left(\frac{M}{1M_\odot}\right)^{1/10}\left(\frac{\varpi}{10^8\,{\rm m}}\right)^{-3/10}\,{\rm kg\,m^{-2}}. \tag{8.16}$$

$$T_c = \left(\frac{3c}{4\sigma_{\rm SB}}\right)^{1/4}\Omega^{1/2}H^{1/4}\sigma^{1/4}, \tag{8.17}$$

ie

$$T_c = 2.0\times10^5\times\alpha^{6/25}\times\left(\frac{\dot{M}f^4}{10^{13}\,{\rm kg/\,s}}\right)^{4/25}\left(\frac{M}{1M_\odot}\right)^{11/80}\left(\frac{\varpi}{10^8\,{\rm m}}\right)^{-33/80}\,{\rm K}. \tag{8.18}$$

8.2 Time-dependent discs

We make use of the continuity equation,

$$\frac{\partial \sigma}{\partial t} + \frac{1}{\varpi}\frac{\partial}{\partial \varpi}\left(\varpi v_\varpi \sigma\right) = 0. \tag{8.19}$$

Angular momentum conservation (with vertical field):

$$\frac{\partial}{\partial t}\left(\sigma \varpi^2 \Omega\right) + \frac{1}{\varpi}\frac{\partial}{\partial \varpi}\left(\varpi^3 \sigma v_\varpi \Omega - \nu\sigma\varpi^3 \frac{\partial \Omega}{\partial \varpi}\right) = 2\varpi \frac{B_z B_\phi^+}{\mu_0}, \tag{8.20}$$

$$\frac{\partial}{\partial t}\left(\sigma \varpi^2 \Omega\right) + \frac{1}{\varpi}\frac{\partial}{\partial \varpi}\left[\left(\varpi\sigma v_\varpi\right)\left(\varpi^2\Omega\right)\left(\nu\sigma\right)\left(\varpi^2\Omega\right)\frac{\partial \ln \Omega}{\partial \ln \varpi}\right] = 2\varpi \frac{B_z B_\phi^+}{\mu_0}, \tag{8.21}$$

$$\begin{aligned}\left(\varpi^2\Omega\right)\left[\frac{\partial \sigma}{\partial t} + \frac{1}{\varpi}\frac{\partial}{\partial \varpi}\left(\varpi v_\varpi \sigma\right)\right] + \sigma \frac{\partial}{\partial t}\left(\varpi^2\Omega\right) \\ + \left(\varpi\sigma v_\varpi\right)\frac{1}{\varpi}\frac{\partial}{\partial \varpi}\left(\varpi^2\Omega\right) - \frac{1}{\varpi}\frac{\partial}{\partial \varpi}\left(\nu\sigma\left(\varpi^2\Omega\right)\frac{\partial \ln \Omega}{\partial \ln \varpi}\right] = 2\varpi \frac{B_z B_\phi^+}{\mu_0}.\end{aligned} \tag{8.22}$$

The first term vanishes because of the continuity equation. Assuming now perfectly keplerian rotation, $\Omega = \Omega_K$, the second term also vanishes, so we have

$$\left(\varpi\sigma v_\varpi\right)\frac{1}{\varpi}\frac{\partial}{\partial \varpi}\left(\varpi^2\Omega_K\right) - \frac{1}{\varpi}\frac{\partial}{\partial \varpi}\left[\nu\sigma\left(\varpi^2\Omega_K\right)\frac{\partial \ln \Omega_K}{\partial \ln \varpi}\right] = 2\varpi \frac{B_z B_\phi^+}{\mu_0}. \tag{8.23}$$

Dividing through by $\Omega = \Omega_K$ yields the equation in the form

$$\left(\varpi\sigma v_\varpi\right)\frac{\partial}{\partial \ln \varpi}\ln\left(\varpi^2\Omega_K\right) - \frac{1}{\varpi^2\Omega_K}\frac{\partial}{\partial \ln \varpi}\left[\nu\sigma\left(\varpi^2\Omega_K\right)\left(-\tfrac{3}{2}\right)\right] = 2\varpi \frac{B_z B_\phi^+}{\mu_0 \Omega_K}, \tag{8.24}$$

$$\tfrac{1}{2}\left(\varpi\sigma v_\varpi\right) + \tfrac{3}{2}\varpi^{-1/2}\frac{\partial}{\partial \ln \varpi}\left[\varpi^{1/2}\nu\sigma\right] = 2\varpi \frac{B_z B_\phi^+}{\mu_0 \Omega_K}. \tag{8.25}$$

Multiply by 2,

$$\varpi\sigma v_\varpi = -3\varpi^{1/2}\frac{\partial}{\partial \varpi}\left[\varpi^{1/2}\nu\sigma\right] + 4\varpi \frac{B_z B_\phi^+}{\mu_0 \Omega_K}. \tag{8.26}$$

So the continuity equation becomes

$$\frac{\partial \sigma}{\partial t} = \frac{1}{\varpi}\frac{\partial}{\partial \varpi}\left[3\varpi^{1/2}\frac{\partial}{\partial \varpi}\left(\varpi^{1/2}\nu\sigma\right) - 4\varpi \frac{B_z B_\phi^+}{\mu_0 \Omega_K}\right], \tag{8.27}$$

or, in terms of logarithmic derivatives,

$$\frac{\partial \ln \sigma}{\partial t} = \frac{3\nu}{\varpi^2}\left(\tfrac{1}{2}A + A^2 + \frac{\partial^2 \ln \nu}{\partial \ln \varpi^2} + \frac{\partial^2 \ln \sigma}{\partial \ln \varpi^2}\right) - \frac{4}{\varpi}\frac{\partial}{\partial \varpi}\left(\varpi \frac{B_z B_\phi^+}{\mu_0 \Omega_K}\right), \tag{8.28}$$

where

$$A = \frac{\partial \ln \nu}{\partial \ln \varpi} + \frac{\partial \ln \sigma}{\partial \ln \varpi}. \tag{8.29}$$

8.3 Modified iteration scheme for h

Instead of iterating with respect to a solution for the electron scattering opacity used by BC we now iterate with respect to a Kramer opacity solution. Thus, instead of having (30) in BC we have now

$$T_c^{15/2} = \frac{27\kappa_{\rm Kr}}{32\sigma_{\rm SB}}\,\alpha\sigma^3\Omega^3 h\left(1+\tfrac{16}{9}{\rm Pr}_M^{-1}\beta^{-1}\right)\left(1+\frac{\kappa_{\rm es}}{\kappa_{\rm Kr}}\right). \tag{8.30}$$

With this we have now instead of (31) in BC

$$h^{14} = \tilde{\mathcal{K}}\alpha\sigma^3\Omega_{\rm K}^{-12}\tilde{\mathcal{C}}, \tag{8.31}$$

where

$$\tilde{\mathcal{K}} = \frac{27\kappa_{\rm Kr}}{32\sigma_{\rm SB}}\left(\frac{2\mathcal{R}}{\mu_{\rm gas}}\right)^{15/2} \tag{8.32}$$

$$\tilde{\mathcal{C}} = \left(1+\tfrac{16}{9}{\rm Pr}_M^{-1}\beta^{-1}\right)\left(\frac{1+\beta_r^{-1}}{1+\beta^{-1}}\right)^{15/2}\left(1+\frac{\kappa_{\rm es}}{\kappa_{\rm Kr}}\right) \tag{8.33}$$

Contents